

# Sexually selected differences in warbler plumage are related to a putative inversion on the Z chromosome

Peter O. Dunn<sup>1</sup>  | Nicholas D. Sly<sup>1</sup> | Corey R. Freeman-Gallant<sup>2</sup> |  
Amberleigh E. Henschen<sup>1</sup> | Christen M. Bossu<sup>3</sup> | Kristen C. Ruegg<sup>3</sup> | Piotr Minias<sup>4</sup> |  
Linda A. Whittingham<sup>1</sup> 

<sup>1</sup>Department of Biological Sciences, University of Wisconsin-Milwaukee, Milwaukee, Wisconsin, USA

<sup>2</sup>Department of Biology, Skidmore College, Saratoga Springs, New York, USA

<sup>3</sup>Department of Biology, Colorado State University, Ft. Collins, Colorado, USA

<sup>4</sup>Department of Biodiversity Studies and Bioeducation, Faculty of Biology and Environmental Protection, University of Łódź, Łódź, Poland

## Correspondence

Peter O. Dunn, Department of Biological Sciences, University of Wisconsin-Milwaukee, Milwaukee, WI 53201, USA. Email: [pdunn@uwm.edu](mailto:pdunn@uwm.edu)

## Funding information

National Geographic Society, Grant/Award Number: WW-202R-17; Narodowe Centrum Nauki, Grant/Award Number: 2015/19/D/NZB/01310; Division of Integrative Organismal Systems, Grant/Award Number: IOS-1749052, IOS-1601093 and IOS-1749044; Division of Environmental Biology, Grant/Award Number: DEB-1942313

Handling Editor: Tatiana Giraud

## Abstract

Large structural variants in the genome, such as inversions, may play an important role in producing population structure and local adaptation to the environment through suppression of recombination. However, relatively few studies have linked inversions to phenotypic traits that are sexually selected and may play a role in reproductive isolation. Here, we found that geographic differences in the sexually selected plumage of a warbler, the common yellowthroat (*Geothlypis trichas*), are largely due to differences in the Z (sex) chromosome (males are ZZ), which contains at least one putative inversion spanning 40% (31/77 Mb) of its length. The inversions on the Z chromosome vary dramatically east and west of the Appalachian Mountains, which provides evidence of cryptic population structure within the range of the most widespread eastern subspecies (*G. t. trichas*). In an eastern (New York) and western (Wisconsin) population of this subspecies, female prefer different male ornaments; larger black facial masks are preferred in Wisconsin and larger yellow breasts are preferred in New York. The putative inversion also contains genes related to vision, which could influence mating preferences. Thus, structural variants on the Z chromosome are associated with geographic differences in male ornaments and female choice, which may provide a mechanism for maintaining different patterns of sexual selection in spite of gene flow between populations of the same subspecies.

## KEYWORDS

birds, inversions, mate choice, phylogeography, sex chromosome, sexual selection, speciation

## 1 | INTRODUCTION

Recent studies have revealed that ecological and morphological differences between closely related species or populations are often associated with large-scale structural variants in the genome, such as inversions or duplications (e.g. copy number variation). Large-scale inversions, for example, average 8.4 megabases (Mb; Wellenreuther & Bernatchez, 2018), are typically much larger than the 'islands of divergence' (regions of high  $F_{ST}$ ) found in earlier genome scans, which are on the order of kilobases, and are often more widely distributed

throughout the genome (Lamichhaney & Andersson, 2019). Structural variants have been relatively unexplored until recently, because detecting them is difficult without highly contiguous genome assemblies (e.g. chromosome level). Structural variants are potentially important for understanding adaptation and evolution, because they have been associated with morphological and behavioural differences that lead to local adaptation (Wellenreuther & Bernatchez, 2018). For example, inversions have been associated with adaptation to freshwater in sticklebacks (Jones et al., 2012), elevation in babblers (Lu et al., 2023), mimetic wing patterns in *Heliconius* butterflies (Jay et al., 2021), type

of shore habitat in snails (Westram et al., 2018) and water depth in fish (Barth et al., 2019). Inversions are thought to facilitate local adaptation by suppressing recombination, leading to reduced gene flow and the maintenance of locally favoured alleles. These processes could also be important during the early stages of speciation (Wellenreuther & Bernatchez, 2018).

Theory and empirical studies suggest that inversions accumulate more often on sex chromosomes over evolutionary time (Charlesworth et al., 1987; Hooper et al., 2019; Irwin, 2018), and if these differences vary geographically, then they could be an important contributor to reproductive isolation of populations. However, in several cases morphological differences between populations and closely related species are associated with inversions on autosomes or a relatively small number of SNPs that control coloration, and thus, it is not clear what role inversions may play in reproductive

isolation and phenotypic differences. For example, a large inversion (115 Mb) on Chromosome 1 of common quail (*Coturnix coturnix*) is associated with two different forms that differ in both plumage colour and migration distance, which leads to geographically discrete distributions for birds with the inversion (Sanchez-Donoso et al., 2021). However, both forms of quail commonly interbreed and the fitness consequences of these differences are not yet known. Alternatively, some large inversions (e.g. 'super-genes') on the autosomes of birds, such as ruffs (*Calidris pugnax*; Kupper et al., 2015) and white-throated sparrows (*Zonotrichia albicollis*; Tuttle et al., 2016), are associated with morphs that have different plumages, and individuals homozygous for the inversion may incur lower fitness. There have also been several recent studies comparing closely related species that are generally similar across the genome except for small regions with a few genes that control species-specific differences in coloration,

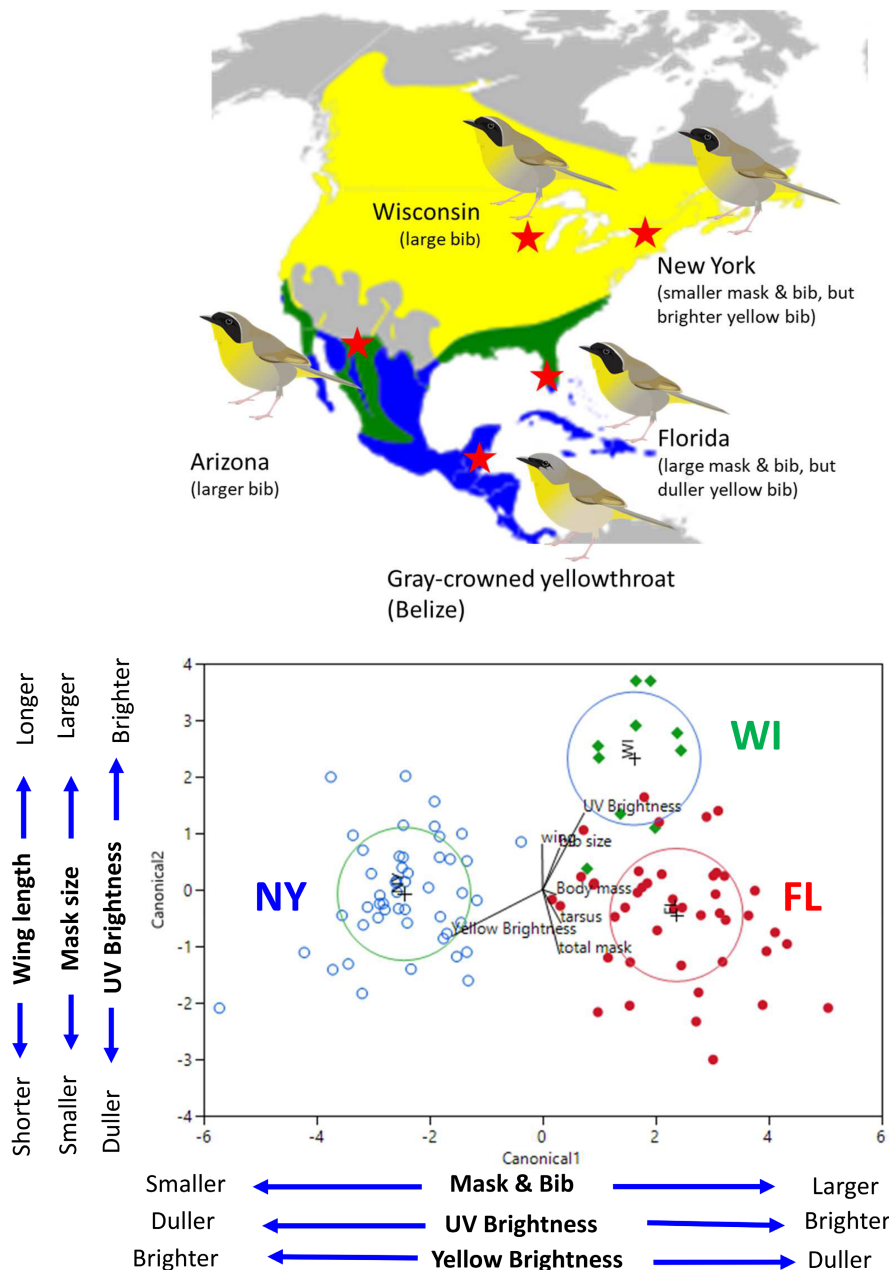


**FIGURE 1** Distribution (top) and morphology (bottom) of common yellowthroats. Top panel shows the breeding (yellow), year-round (green) and winter (blue) range of common yellowthroats (Wikipedia) and the location of our main study populations (red stars). Wisconsin and New York populations are the same subspecies (*Geothlypis trichas trichas*), while the Florida (*G. t. ignota*) and Arizona (*G. t. chryseola*) populations are different (non-migratory) subspecies. We also studied the grey-crowned yellowthroat (*G. poliocephala palpebralis*) in Belize, which has a small mask and grey head (sexes are similar in plumage). Bird illustrations by Jess McLaughlin. Bottom panel shows a discriminant function analysis of the morphology of males in Florida, New York and Wisconsin populations using mask and bib size, wing length, body mass and brightness in the ultraviolet (UV) and yellow portions of the spectrum (see Section 2). These data are from Whittingham et al., 2018. [Colour figure can be viewed at [wileyonlinelibrary.com](https://onlinelibrary.wiley.com/doi/10.1111/mec.17525)]

particularly genes in melanin pathways that produce black and brown pigments (Knief et al., 2019; Poelstra et al., 2014; Toews et al., 2016; Wang et al., 2020). In many of these studies, the comparisons are between well-defined species, so it is often not clear if these areas of genomic divergence (inversions or smaller regions) arose early in the process of speciation during changes in pre-zygotic isolating mechanisms (e.g. changes in mate choice before extensive divergence) or later in speciation during changes in post-zygotic mechanisms, perhaps after secondary contact. Theory suggests that larger inversions should form early in the speciation process, partly because they prevent recombination from breaking up adaptive allele combinations (Schaal et al., 2022); however, several empirical studies suggest that inversions are often relatively old (>100K generations) and may have evolved in allopatry (Wellenreuther & Bernatchez, 2018). Thus, studying genomic divergence in species at the earliest stages of reproductive isolation may help to understand the early stages of speciation.

In this study, we examine a sexually dichromatic warbler (Parulidae) with several subspecies that are similar in appearance and potentially at these early stages of speciation. The common yellowthroat (*Geothlypis trichas*) breeds across most of the United States (US) and southern Canada (Figure 1) and has 13 subspecies (Guzy & Ritchison, 1999) in which males possess a black melanin-based facial mask and a yellow carotenoid-based throat and breast ('bib'; Figure 1). Females lack the black mask and typically have a smaller and more subdued bib. Variation in the size and shape of the black mask and yellow throat ornaments in males has evolved relatively recently across subspecies (within the last 1 My; Escalante et al., 2009). These ornaments are likely subject to strong sexual selection, which may have influenced their rapid divergence. Our previous research on two populations within one subspecies of common yellowthroat (*G. trichas trichas*) has revealed strong, but divergent, sexual selection on the black mask and yellow bib. Notably, females prefer males with larger black masks in a Wisconsin (WI) US population, while females in a New York (NY) US population prefer males with larger and brighter yellow bibs (Dunn et al., 2008). Interestingly, the female-preferred ornaments are each honest indicators of male quality in their respective populations, but not vice versa (Freeman-Gallant et al., 2010; Whittingham et al., 2015). Change in preference alongside change in the size or colour of preferred ornaments may be a path to diversification in a group of otherwise ecologically similar taxa (Mendelson et al., 2014; Servedio & Boughman, 2017; Wellenreuther et al., 2014, 2019).

If sexual selection on plumage ornaments is an important contributor to the diversification of yellowthroats, then we can expect genes associated with ornament production and female preference to be among the most divergent genomic regions in comparisons between populations. Here, we examined genomic differences between populations of yellowthroats that differ widely in plumage (Figure 1). Our comparisons included different populations of the same subspecies (e.g. NY vs. WI; *G. trichas trichas*), as well as comparisons between subspecies (e.g. NY vs. Florida [FL]; *G. t. trichas* vs. *G. t. ignota*) and another *Geothlypis* species (grey-crowned

yellowthroat, *Geothlypis poliocephala palpebralis*) that is sexually monomorphic and presumably subject to less intense sexual selection on plumage ornaments. Our initial comparisons of the NY and WI populations revealed a large putative inversion on the Z chromosome (males are ZZ and females are ZW in birds), which we examined further to determine its geographic extent and role in plumage differentiation. In particular, we tested whether the Z chromosome was more closely related to morphological differences between populations than the autosomes. Lastly, we identified outlier genes on the Z chromosome and compared them to candidate genes previously associated with pigmentation or ornament size. Our results suggest that genetic differentiation during the early (and cryptic) stages of speciation may be related to large inversions that affect morphology and behaviour, particularly on the sex (Z) chromosome.

## 2 | METHODS

### 2.1 | Sample collection

Our initial analysis examined sequences from pooled DNA samples ('pool-seq'; Schlotterer et al., 2014) from four populations of common yellowthroats (*Geothlypis trichas*) in the United States and one population of the closely related grey-crowned yellowthroat (*Geothlypis poliocephala palpebralis*) from Belize (Figure 1). The four common yellowthroat populations included one subspecies, *G. trichas trichas* from Wisconsin (WI) and New York (NY), and two other subspecies from Florida (*G. t. ignota*, FL) and Arizona (*G. t. chryseola*, AZ). These populations vary in mask and bib size (Figure 1), and represent an increasing gradient of genetic divergence from differences between one subspecies to differences between subspecies and species. The FL and AZ subspecies are also non-migratory, in contrast to *G. t. trichas* in NY and WI, which migrate to the southern United States and Mexico in the winter. We collected samples from yellowthroats in these populations on breeding territories using mist-nets and took morphometric measurements and blood samples for DNA analysis (for more details see Freeman-Gallant et al., 2010; Whittingham et al., 2018). All captured birds were subsequently released unharmed, and all animal care use was approved by Institutional Animal Care and Use Committees at Skidmore College (163) and the University of Wisconsin-Milwaukee (11-12 #33, 15-16 #42, 17-18 #31). Blood samples from AZ, FL and Belize were collected and imported under permits (see Section Acknowledgments).

Following the discovery of a putative inversion, we expanded our analysis to include additional samples from individuals (i.e. not pooled samples) to determine the geographic extent of the inversion. These individuals were sequenced at low coverage across their genomes as part of the Bird Genoscape Project ([www.birdgenoscape.org](http://www.birdgenoscape.org)), which maps genetic variation across the range of species to study connectivity and migratory pathways. Captures of banded individuals in the east suggest that common yellowthroats generally migrate north and south and infrequently cross over the

Appalachian Mountains (24% [18/74] of recaptures; Figure S1), so we hypothesized that these mountains were a barrier to gene flow that might result in geographic structure. We included 100 samples of *G. t. trichas* that were from locations primarily west (Kansas, KS; Kentucky, KY; Michigan, MI; New York, NY; Ontario, ON; Quebec, QC) and east of the Appalachian Mountains (New Brunswick, NB; Pennsylvania, PA), or in the southeast where there are two different subspecies: *G. trichas typhicola* in Alabama (AL) and North Carolina (NC) and the resident subspecies, *G. trichas ignota*, in Florida. More details of the locations and analyses of samples are in Table S1 and Dunn et al. (2023).

## 2.2 | Ornament size and colour

We measured ornament (mask and bib) size of males in FL, NY and WI (Figure 1) by photographing captured males in standardized postures against a background of 1 cm<sup>2</sup> to capture images of the mask (both sides of the head) and bib. These pictures were imported into ImageJ (<http://imagej.nih.gov/ij/>) and scaled to a 1 cm<sup>2</sup> grid in each picture. We measured ornament size of males by tracing the outlines of the bib and mask (both sizes summed) in ImageJ. Estimates were averaged from two sets of pictures. Repeatabilities of these measurements are >0.90 for different pictures and different persons performing the measurements (Freeman-Gallant et al., 2010). To measure coloration of the yellow bib (breast), we measured the reflectance of feathers using an Ocean Optics 2000 UV-VIS spectrophotometer (for details, see Freeman-Gallant et al., 2010). In this study, we only had feathers available from males in FL, NY and WI, and we focus on brightness in the ultraviolet (320 to 400 nm) and yellow (550 to 625 nm) portions of the spectrum, which was estimated by average reflectance. To examine morphological differences between the common yellowthroat populations, we used mask and bib size, wing length and body mass as predictors in a principal component analysis (PCA) in JMP v.16 (SAS Institute, 2020). For the analysis of the FL, NY and WI populations, we also added UV and yellow brightness as predictors in the analysis.

## 2.3 | DNA extraction and sequencing

DNA was extracted using the Qiagen DNeasy Blood and Tissue kit (cat no.: 69504; Qiagen, Valencia CA).

We constructed genomic DNA pools for pooled sequencing ('pool-seq'; Schlotterer et al., 2014) of our four main common yellowthroat populations (i.e., AZ, FL, NY and WI) and the grey-crowned yellowthroat (Table S1). The concentration of extracted DNA was measured using NanoDrop and Qubit fluorometers, and then, the individual DNA samples were pooled ( $N=36$  to 40 individuals) with equal starting amounts of total DNA per individual in the pool. The individuals in these genomic pools were a random selection of individuals; however, for some analyses, we also used pools of males

from NY and WI that we previously analysed in terms of ornament size (Sly et al., 2022). These NY and WI pools consisted of individuals with relatively large (top 25% of the size distribution) or small (bottom 25%) mask or bib ornaments. Comparisons of these pools allowed us to isolate genes related to ornament size and not geographic differences. All pools contained only males, except the grey-crowned yellowthroat pool which contained 23 males, 12 females and 1 unknown sex, because males and females are similar in plumage. The pooled samples were checked for quality and concentration and then sequenced on an Illumina HiSeq by the University of Wisconsin Madison Biotechnology Center or Novogene Corporation (Sacramento, CA). For the individual whole-genome samples, we used blood or feather tips to make whole-genome sequencing libraries (Nextera Library Preparation protocol; Illumina Corporation), which were sequenced by Novogene Corporation to an average of 2.9× coverage.

## 2.4 | Sequence filtering and alignment

For pool-seq samples, we used Trimmomatic (v. 0.39, Bolger et al., 2014) to remove Illumina adapter sequences, trim leading and trailing bases with quality scores below 3, and use a 4-base sliding window to trim reads when the average quality dropped below a score of 15. We dropped reads less than 36 bases in length and retained paired reads. These steps resulted in the retention of an average 96% of read pairs per pool.

We aligned paired and trimmed reads to a reference genome of the common yellowthroat using bwa mem with default settings (v 0.7.17; Li & Durbin, 2010). The reference genome (GCA\_009764595.1) was constructed by the G10K-Vertebrate Genomes Project (PRJNA589703) using a DNA sample collected from a female at our WI study site (Sly et al., 2022). The genome was assembled (VGP pipeline 1.5, Rhie et al., 2020) using a combination of long and short reads and optical mapping techniques (52× coverage using PacBio Sequel I CLR, Illumina NovaSeq, Arima Genomics Hi-C and Bionano Genomics DLS technology) and curated with gEVAL (Howe et al., 2021), which uses the optimal mapping data to identify and correct local assembly errors. The common yellowthroat reference genome was 1.078 Gb with 52× coverage, a scaffold N50 of 72.5 Mb and contig N50 of 3.25 Mb on 32 autosomal chromosomes, W and Z sex chromosomes and 242 unplaced scaffolds. The Z and W chromosome assemblies of common yellowthroats were 88 and 86% identical to the respective assemblies of the zebra finch (GCF\_003957565.2), which was assembled with a similar VGP pipeline (v. 1.7, see Figure S2). Synteny analysis of the common yellowthroat and zebra finch genomes with fastANI (v. 1.33, Jain et al., 2018) did not reveal any misassembly between the sex chromosomes (Figure S2). After alignment of reads to the reference genome, we dropped reads with a quality score below 20 and converted the SAM files to BAM format using samtools (v1., Danecek et al., 2011). These steps resulted in aligned pools with an average genomic read depth of 40.6×.

## 2.5 | Patterns of population divergence, diversity and selection

We initially used  $F_{ST}$  to screen the genome for regions of elevated differentiation that might be caused by mechanisms that reduce gene flow such as inversions or different types of selection.  $F_{ST}$  is a relative measure of population differentiation, so it can be elevated because of either large differences in diversity between populations or lower variation within a population (Cruickshank & Hahn, 2014). Thus, we also examined an absolute measure of divergence, the average number of pairwise differences between sequences from two populations,  $\pi_{\text{Between}}$  (Nei & Li, 1979; also known as  $d_{XY}$  or  $\pi_{XY}$ ), and the pairwise difference between sequences within the same population ( $\pi_{\text{Within}}$ ).  $F_{ST}$  is directly related to  $\pi_{\text{Within}}$  and  $\pi_{\text{Between}}$  (see Figure 1 in Cruickshank & Hahn, 2014), and hence, these two measures of divergence provide some insight into the source of elevated levels of  $F_{ST}$  and the likely model of differentiation. For example, some regions of elevated  $F_{ST}$  appear to be due to relatively low  $\pi_{\text{Within}}$  in the same genomic region. This pattern has been observed in comparisons of other pairs of warbler species or subspecies and has been attributed to episodes of selection that reduce  $\pi_{\text{Within}}$  relatively more than  $\pi_{\text{Between}}$  (see Figure 6 in Irwin et al., 2018).

We used PoPoolation2 (v 1.201, Kofler et al., 2011a) to compute  $F_{ST}$  between each pair of population pools. These pairs of files were constructed by converting BAM files for each population pool into mpileup files using samtools, and then combining pairs of mpileup files into sync files using the mpileup2sync java script from Popoolation2. We computed  $F_{ST}$  values for non-overlapping 20 kilobase windows between pools using the PoPoolation2 scripts fisher-test.pl and fst-sliding.pl. These scripts were run using a minimum allele count of 4, a minimum read depth of 10, a maximum read depth of 3X the genomic mean depth (averaged between the two pools being compared), and a minimum covered fraction of the window of 0.1.  $D_{XY}$  was calculated from the same sync files using a script (sync2dxy.pl) at [https://github.com/owensgl/pop\\_gen](https://github.com/owensgl/pop_gen), which implements the formula:  $(p1 \times q2) + (p2 \times q1)$ , where  $p1$  and  $q1$  are the frequencies of the two alleles in one population and  $p2$  and  $q2$  are the frequencies of the same alleles in the second population. We calculated nucleotide diversity ( $\pi$  or  $\pi_{\text{Within}}$ ) for each pool individually from mpileup files (created with non-overlapping 20-kb windows using the variance-sliding.pl script from PoPoolation v.1.2.2, Kofler et al., 2011b) with a minimum allele count of 2 and the same depth parameters as for  $F_{ST}$ . We also used the variance-sliding.pl script and the same parameters to estimate Tajima's  $D$ , which provides information on whether selection or reduced gene flow may be producing regions of increased  $F_{ST}$  divergence. A negative Tajima's  $D$  value indicates an excess of rare alleles, which may be due to a recent selective sweep or a population expansion, while a positive  $D$  value indicates a scarcity of rare alleles which may be due to balancing selection or a bottleneck.

To help distinguish positive selection from genome-wide selection and to estimate the intensity of selection at individual loci, we used SelEstim (v.1.1.7, Vitalis et al., 2014), which accepts pool-seq

data and is based on a hierarchical Bayesian model in which all loci are assumed to be responding to selection to some extent. The model is based on a diffusion approximation of the distribution of allele frequencies in a Wright–Fisher island model. SelEstim uses a Markov chain Monte Carlo (MCMC) algorithm to sample from the posterior distribution of model parameters. Loci under selection are identified using the 1% threshold level of Kullback–Leibler divergence (KLD), which compares the selection estimate at a locus with a ‘centring distribution’ of genome-wide selection estimates. For our comparison of populations, we used 25 pilot runs of 500 iterations each to adjust the distributions for each model parameter and, after a 100,000 burn-in period, 10,000 MCMC samples of 500,000 length were performed with a thinning interval of 50, yielding 10,000 observations.

We also examined linkage disequilibrium (LD) between and within some populations to help identify potential inversions. If all or most individuals in a population share the same inversion type, then there should be reduced recombination (and higher LD) between inversion types in different populations, but typical rates of recombination (and LD) within populations with the same inversion type (see also McCallum et al., 2024). For this analysis, we calculated LD using PLINK (v 1.9; Purcell et al., 2007) and SNP data obtained from double-digest restriction site-associated DNA (ddRAD) sequences of individuals in our previous study of the New York ( $n=36$ ) and Wisconsin ( $n=46$ ) populations (Table S1; Whittingham et al., 2018). We used ddRAD data and PLINK in this analysis, rather than pool-seq data, because LD cannot usually be calculated beyond the length of a read pair with pool-seq data. However for visualizing LD on the Z chromosome, we also included estimates of LD for pool-seq data based on LDx (Feder et al., 2012). LDx uses a maximum-likelihood approach to estimate LD between pairs of single-nucleotide polymorphisms (SNP) within and among single sequencing reads. SNPs were read from variant call format (VCF) files that were constructed from the BAM files above with bcftools (v 1.10, Danecek et al., 2011). We computed non-overlapping 20-kb windows of linkage disequilibrium across the chromosome by taking the mean  $r^2$  values between SNPs that were 25–75 bp apart (low coverage pools) or SNPs 100–200 bp apart (high coverage pools) within each window (filtering for a minimum read depth of 10 and a maximum read depth of 3x the genomic mean depth for a given pool).

We initially analysed population divergence by plotting  $F_{ST}$  in Manhattan plots using the qqman package in R. We identified outlier regions for each population comparison as those in the top 1% of autosomal  $F_{ST}$  windows (20 kb). We also produced heatmaps of  $F_{ST}$  in the R package poolFstat (Gautier et al., 2022). For the pool-seq samples, we conducted PCA with poolFstat, which we also used to extract allele frequencies (from the poolFstat data object). These allele frequencies were input to pcaAdapt (v 3.0.2, Luu et al., 2017) to conduct a component-wise PCA, which calculates correlations (loadings) between each SNP and individual PCA axes (see Section 2.7 below). We also used poolFstat to export an input file for BayPass (v 2.3, Gautier, 2015), which we used to construct separate hierarchical clustering trees for the autosomes and Z chromosome. BayPass

uses a Bayesian hierarchical model to estimate a scaled covariance matrix of population allele frequencies, which accounts for the neutral correlation of allele frequencies across populations. The BayPass analysis was conducted using default parameters on files thinned to 1 SNP per 1000 using vcftools to account for linkage disequilibrium. The covariance matrix output from BayPass was then imported into R and converted into a correlation matrix for plotting the trees using utilities included in the BayPass software.

## 2.6 | Detecting inversions and their geographic extent

The initial analysis of  $F_{ST}$  using the pooled samples revealed a large outlier region on the Z chromosome, which may be due to an inversion. Inversions are commonly found on the Z chromosome in birds (Hooper & Price, 2017; Yazdi & Ellegren, 2018). Using the pooled samples, we identified breakpoints for putative inversions with LUMPY (Layer et al., 2014), which achieves high precision identifying inversions by using several different signals from sequence alignments (read depth and the distribution of read pairs; Mahmoud et al., 2019).

Next, to determine the geographic extent of the putative inversion on the Z chromosome (see Section 3), we examined  $F_{ST}$  and admixture with whole-genome samples from individuals in the eastern part of the range (see above and Table S1). If the putative inversion is primarily related to differences between populations east and west of the Appalachian Mountains, then we would expect to see larger  $F_{ST}$  values in comparisons of birds east and west of the Appalachian Mountains on the Z chromosome than on the autosomes. Similarly, we should see stronger population structure on the Z chromosome than the autosomes when comparing samples from east and west of the Appalachian Mountains. To study population structure in these samples, we used the program admixture (Alexander et al., 2009), which uses a maximum-likelihood approach to estimate population ancestry. The whole-genome sequences were processed similarly to the pool-seq sequences, although trimming was performed with TrimGalore (Krueger, 2020), and we made VCF files using the GATK variant discovery pipeline (van der Auwera & O'Connor, 2020) (<https://gatk.broadinstitute.org/hc/en-us/articles/360035890411?id=3893>). Using vcftools (Danecek et al., 2011), we further filtered the VCF files for minor allelic frequency ( $maf=0.05$  and  $max-maf=0.95$ ) and quality ( $q=30$ ) and only included biallelic SNPs found in at least 75% of individuals. For the admixture analysis, the VCF file was also thinned with vcftools to one SNP per 1000 base pairs to remove linked loci.

## 2.7 | The role of the Z chromosome and inversions in plumage differences

To examine the role of the Z and its putative inversion in plumage evolution, we tested which chromosomes (Z or autosomes) were

more closely related to morphological differences between and within populations. Here, we conducted two sets of analyses. The first analysis used the pooled samples and component-wise PCA with pcaAdapt (v 3.0.2, Luu et al., 2017), which calculates correlations (loadings) between each SNP and individual PCA axes (i.e., morphology). In this case, the axes were based on populations that differ in size and colour (Figure 1). We then compared these correlations on the Z chromosome and autosomes using Wilcoxon tests in JMP v. 16 (SAS Institute, 2020) to determine whether genomic differences between populations (along a PCA axis) were more closely associated with the Z chromosome or autosomes.

Our second analysis was a GWAS that used data from individual birds and compared the number of significant associations between morphology and SNPs on each type of chromosome (Z or autosomes) using a linear mixed model (lmm) in GEMMA v0.98.5 (Zhou & Stephens, 2014). These SNP data were obtained from the ddRAD sequences of individuals in our previous study of the New York ( $n=36$ ) and Wisconsin ( $n=46$ ) populations (Table S1; Whittingham et al., 2018). We used these samples so we could obtain morphological measurements of individuals, including both ornament size and colour, which were unavailable for the other samples (pool-seq and whole genome). We also focused on the NY and WI samples because they are the same subspecies (*G. t. trichas*), and thus, geographic variation is reduced compared with analyses between subspecies. The ddRAD sequences were obtained following the protocol of Peterson et al. (2012) and additional details of library preparation and sequencing are in Whittingham et al. (2018). In this study, we mapped those sequences to the common yellowthroat reference genome (as above) and used the STACKS pipeline (Catchen et al., 2013) to produce VCF files. These files were filtered for biallelic alleles that were found in 90% of individuals and had a minor allele frequency >5%. VCF files were imported into PLINK (Purcell et al., 2007) and converted to bed format for analysis of the association between male morphology and each SNP in linear mixed models in GEMMA (Zhou & Stephens, 2014).

If SNPs on the Z chromosome (or its inversion) were more closely related to morphological differences between populations than SNPs on the autosomes, then we expected to find more variation in morphology (PC1) explained by genomic differences (using GEMMA) on the Z chromosome (or the inversion) than on the autosomes. The percentage of variation in PC1 explained by each SNP was calculated as  $2f(1-f)\beta^2$ , where  $f$  is the minor allele frequency and  $\beta$  is the slope estimate from GEMMA for a particular SNP (Sham & Purcell, 2014). These estimates were summed for each chromosome and compared between autosomes and the Z chromosome. Here, we used the first principal component scores of the morphology of individual males in NY and WI as a composite measure of morphology. The PCA contained mask and bib size, wing and tarsus length, body mass and brightness in the ultraviolet (UV) and yellow portion of the spectrum (see Freeman-Gallant et al., 2010 for details of colour measurements). The first PC axis explained 42% of the variation in male morphology (for NY and WI samples together). We used these PC1 scores as the response in a

Imm in GEMMA that tested the association between morphology (PC1) and each ddRAD based SNP on the autosomes, the Z inversion or the rest of the Z chromosome.

## 2.8 | Gene annotation

Using the pool-seq data, we identified outlier genes in the top 1% of  $F_{ST}$  values (in 20kb windows) between populations. Our final list of candidate genes also included all annotated genes within 25kb upstream or downstream of the window. Gene predictions were made from our annotated reference genome of the common yellowthroat (Sly et al., 2022). We tested each candidate gene set for enrichment in Gene Ontology (GO) Biological Process terms using g:Profiler (Raudvere et al., 2019). In addition, we compared divergent genes to lists of candidate genes previously associated with melanin or carotenoid pigmentation in the literature (e.g. Sly et al., 2022), and to lists of candidate genes we previously found associated with ornament size within Wisconsin and New York populations (Sly et al., 2022).

## 3 | RESULTS

### 3.1 | Morphological differences between populations

Populations of common yellowthroats vary in size and colour (Figure 1). Discriminant function analysis was able to distinguish between the FL, NY and WI populations using primarily mask, bib and wing size and UV and yellow brightness (5.8% of samples misclassified; Wilk's  $\Lambda=0.09$ ,  $F=30.8$ ,  $df=14, 188$ ,  $p<.001$ ; Figure 1). Mask size is largest in Florida, followed by WI and NY (all significantly different in Tukey's tests  $\alpha=0.05$ ; Figure S3). Bib and wing size are similar in FL and WI and smaller in NY (Figure 1, Figure S3). In contrast, common yellowthroats in Arizona (*G. t. chryseola*) and grey-crowned yellowthroats in Belize have extensive yellow covering much of the breast and belly. In grey-crowned yellowthroats the mask is also much smaller and the sexes look similar (Figure 1).

### 3.2 | Increasing genomic divergence between populations, subspecies and species of yellowthroats

Genomic divergence among yellowthroat populations forms a gradient at both the autosomes and the Z chromosome, with  $F_{ST}$  increasing in comparisons of pool-seq samples between populations of the same subspecies (WI vs. NY,  $F_{ST}=0.06$ ) to between subspecies (WI and NY vs. FL or AZ; mean  $F_{ST}=0.16$ ) and between species (AZ/FL/NY/WI vs. GC; mean  $F_{ST}=0.57$ ; Figure 2a). A hierarchical clustering tree from BayPass indicated relationships congruent with current taxonomic relationships when using the autosome SNPs (Figure 2b).

For example, NY and WI (the same subspecies) clustered together, followed by decreasing similarity with different subspecies (FL, AZ) and the grey-crowned yellowthroat. In contrast, when analysing SNPs on the Z chromosome, NY and FL clustered together and then WI, AZ and grey-crowned yellowthroat followed in decreasing similarity. Thus, WI was more similar to FL (a different subspecies) than to NY (same subspecies) on the Z chromosome, but more similar to NY than FL on the autosomes.

### 3.3 | Divergence on the Z chromosome

Closer inspection of each chromosome revealed that divergence ( $F_{ST}$ ) between populations was not uniform (Figures S4 and S5), as it was higher on the Z chromosome (mean  $F_{ST}=0.29$ ) than on the autosomes (mean  $F_{ST}=0.01$ ;  $p=.025$ , paired  $t=3.2$ ,  $df=5$  matched pairs excluding GCYE; Figure 2c). The extent of divergence on the Z chromosome varied between populations and regions of the Z chromosome. Divergence ( $F_{ST}$ ) between WI and the other pool-seq populations of common yellowthroats (AZ, FL, NY; Figure 3a) was consistently high in a region spanning ~30.6Mb between 33.8–64.4Mb on the Z chromosome (total length of Z=77Mb). In contrast, comparisons between NY and FL showed a smaller region of divergence, and comparisons of NY with AZ showed a more uniform distribution of elevated  $F_{ST}$  values (Figure 3a). Other comparisons, such as between distant subspecies (FL–AZ) or between species (FL or AZ to grey-crowned yellowthroats), showed widespread divergence, but no specific regions of elevated divergence (Figure S5).

To compare the extent of divergence on the Z chromosome relative to the autosomes, we used the percentage of  $F_{ST}$  outliers (top 1%) between the NY and WI pool-seq populations in windows of 20kb. Overall, outlier  $F_{ST}$  values were not evenly distributed as there was a much greater percentage (40%, 1482/3739) of outlier windows on the Z chromosome than on the autosomes (1%, 472/47240; Figure S4). The annotated genes in these outlier windows for the NY and WI comparison are in Data Table S1 ( $n=763$  autosomal genes) and Data Table S2 ( $n=257$  Z genes) on Dryad (Dunn et al., 2023; <https://doi.org/10.5061/dryad.g1jwstqxd>). We also examined the distribution of fixed differences ( $F_{ST}=1$ ) between the NY and WI populations and their proximity to genes. The majority of fixed SNPs differing between NY and WI (56%, 5140/9137) were found in the region of elevated  $F_{ST}$  on the Z (i.e. the putative inversion, see below), but relatively few of these SNPs were found within genes (12% in the putative Z inversion; 15% on the Z outside the inversion). Fewer fixed SNPs were found on the autosomes (33%, 3055/9137; mean per chromosome: 0.01%, range: 0–7%; Chromosomes 1–31) and 21% of these were within genes. Two of the fixed SNPs between NY and WI were near (<14 Kb) classic melanin-related genes: tyrosinase (TYR) on Chromosome 2 and Tyrosinase-related protein 1 (TYRP1) on the Z chromosome.

In contrast to the elevated  $F_{ST}$  in the middle of the Z chromosome (Figure 3a),  $\pi_{\text{Between}}$  (or  $d_{XY}$ ) did not differ significantly across the autosomes or Z chromosome in any of the paired comparisons

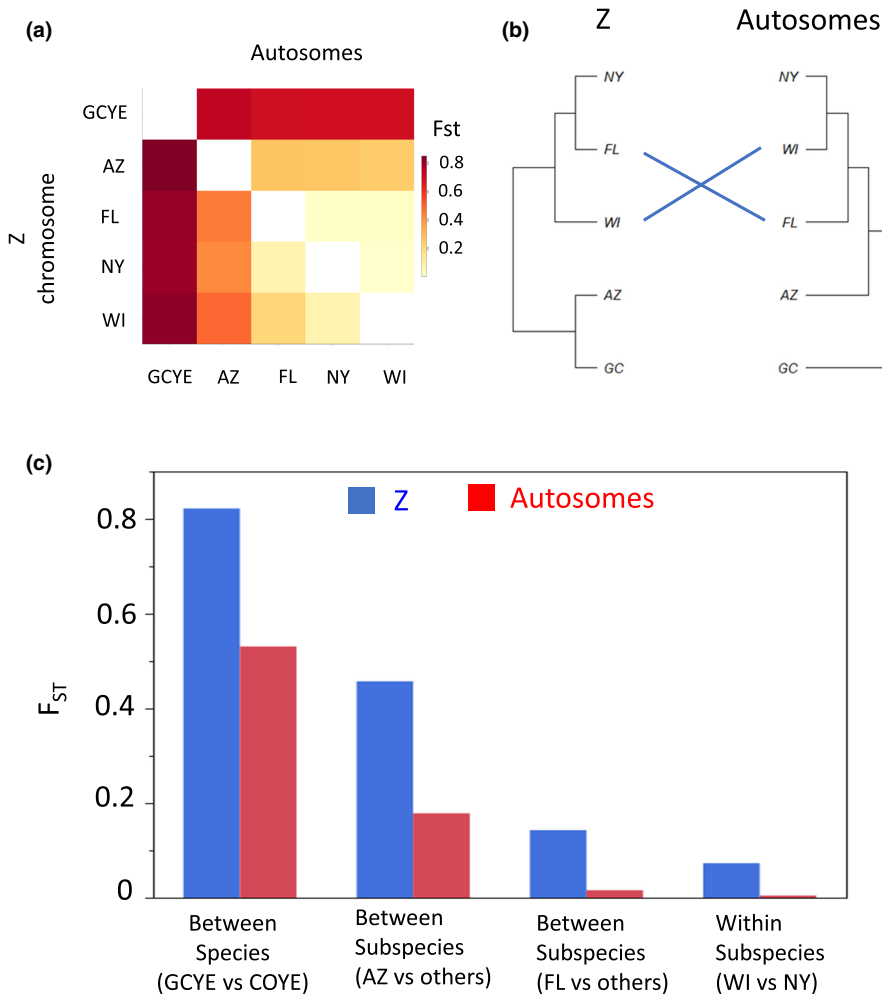


**FIGURE 2** Values of  $F_{ST}$  from pool-seq samples of common and grey-crowned (GC) yellowthroats in all study areas. Panel (a) shows a heatmap constructed with pairwise  $F_{ST}$  values between populations from the Z chromosome (bottom half of matrix) and autosomes (top half) using poolFstat. Panel (b) shows a hierarchical clustering tree from BayPass which shows the change in similarity between NY and WI (the same subspecies) when using SNPs on the Z chromosome (left side) versus autosomes (right side). Panel (c) shows the same  $F_{ST}$  values in Panel (a) averaged for comparisons within and between subspecies and between species (SE based on jackknife estimates using poolFstat were all  $<0.001$  and too small to plot). [Colour figure can be viewed at [wileyonlinelibrary.com](http://wileyonlinelibrary.com)]

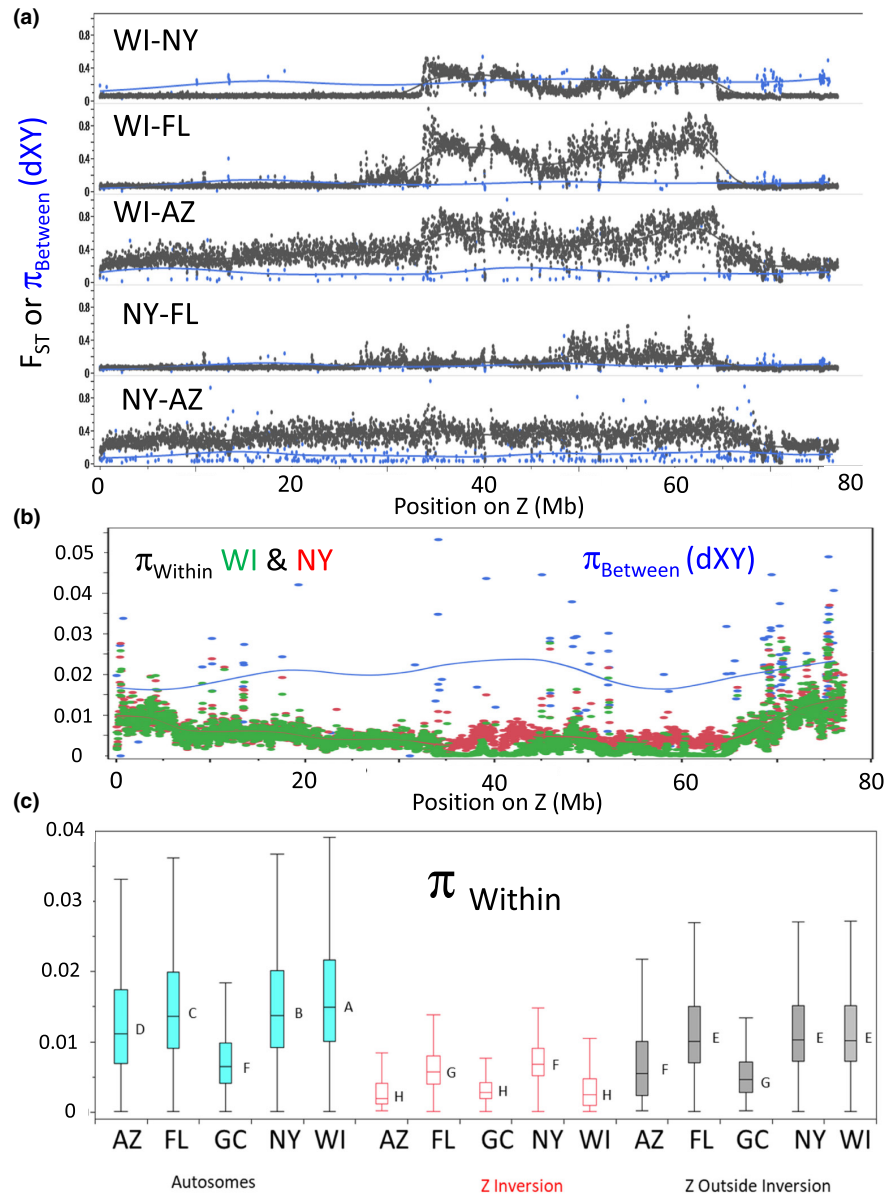
of common yellowthroat populations (Figure 3a,b, Figure S6). The high  $F_{ST}$  values in the comparison of NY and WI populations were primarily due to lower  $\pi_{Within}$  in WI than NY in the elevated  $F_{ST}$  region (Figure 3c); there was little difference in  $\pi_{Between}$  ( $d_{XY}$ ) between the elevated  $F_{ST}$  region and the rest of the Z chromosome (blue line in Figure 3b, Figure S6). This pattern of lower  $\pi_{Within}$  in the elevated  $F_{ST}$  region of the Z chromosome (the putative inversion, see below) was also found in the other populations (Figure 3c, Figure S6).

Based on read position and depth, LUMPY identified three potential inversions on the Z chromosome over 5Mb in length: one 30.6Mb long (starting at 33.8Mb) in FL and NY, a second one in FL 18.8Mb long (starting at 52.2Mb) and a third 5.2 to 6Mb long in all the populations except AZ (starting at ~70Mb; Figure 4a). The breakpoints identified by LUMPY for the 30.6Mb inversion (Figure 4a) coincided with large changes in frequencies of the reference allele, primarily in one direction in WI, which had the reference genome, and the opposite direction in AZ, FL and GCYE; reference allele frequencies were intermediate in frequency in NY (Figure 4b). The WI population also showed lower levels of heterozygosity and higher linkage disequilibrium and Tajima's  $D$  within the inversion starting at 33.5Mb (Figure 4c-f). Consistent with an inversion, there was also a block of higher linkage disequilibrium in the region of the putative inversion when comparing NY and WI populations with a heatmap

(see blue triangle in middle panel of Figure 4d), but relatively low levels when analysing individuals from a single population (NY or WI;  $n=4284$  SNPs found in all three comparisons; Figure 4d).

Analysis of the Z chromosome with SelEstim indicated that the putative inversions were also associated with high levels of positive selection (relative to genome-wide selection). In a comparison of all five pool-seq samples (AZ, FL, NY, WI and grey-crowned yellowthroats), selection averaged higher in the inversion (mean  $\pm$  SE KLD =  $0.286 \pm 0.003$ ,  $n=9172$ ) than outside the inversion (mean  $\pm$  SE KLD =  $0.215 \pm 0.002$ ,  $n=12,072$ ,  $t=16.7$ ,  $df=14,573$ ,  $p<.001$ ) and there were more significant coefficients of positive selection (top 1% of KLD values) in the putative inversion (5.3%, 487/9172) than outside it (0.8%, 90/12,072, Fisher's exact test  $p<.001$ ; Figure S7). A similar pattern occurred in the comparison of NY and WI pools (Figure S7a). In this case, selection was lower overall, but it still averaged higher in the inversion (mean  $\pm$  SE KLD =  $1.19e-3 \pm 1.27e-5$ ,  $n=4581$ ) than outside the inversion (mean  $\pm$  SE KLD =  $1.08e-3 \pm 0.002$ ,  $n=9532$ ;  $t=7.13$ ,  $df=8365$ ,  $p<.001$ ), and there were also more outliers (top 1% of KLD values) inside the putative inversion (1.4% 63/4581) than outside it (0.8%, 75/9532, Fisher's exact test  $p=.0013$ ; Figure S7b). This pattern of stronger selection inside the inversion changed, however, when we examined selection within single populations (Figure S7c, see Section 3.6 below).

**FIGURE 3** Manhattan plots of  $F_{ST}$  (over 20kb windows) on the Z chromosome between pooled samples from common yellowthroats. Comparisons between WI and other areas (a) showed a 31.2 Mb region of high  $F_{ST}$  between 33.5–64.7 Mb on the Z chromosome (total length of Z=77 Mb). In contrast, comparisons between NY and FL showed a smaller region of divergence, and comparisons of NY with AZ showed a more uniform distribution of elevated  $F_{ST}$  values. Additional comparisons of the entire genome are in Figures S4 and S5. Panel (b) shows between-population nucleotide divergence ( $\pi_{\text{Between}}$  or  $d_{XY}$ ) is relatively similar across the Z chromosome, while within-population nucleotide divergence ( $\pi_{\text{Within}}$ ) is lower within the inversion for both NY and WI, but lowest for WI inside the putative inversion. Panel (c) uses boxplots to show  $\pi_{\text{Within}}$  is also lower within the inversion for other pool-seq populations. Letters next to box plots of  $\pi_{\text{Within}}$  indicate populations that are significantly different from a Tukey's test comparing all populations across the autosomes, Z inversion and Z outside the inversion. [Colour figure can be viewed at [wileyonlinelibrary.com](http://wileyonlinelibrary.com)]



### 3.4 | Z inversion is found in other populations west of the Appalachians

To determine the geographic extent of the putative inversion, we examined DNA samples from individual birds throughout the eastern seaboard (Figure 5, Table S1). Here, we started our analysis with the entire Z chromosome because there was some variation in the location of inversions and their size across populations (see Figure 4a). As noted in the Methods (Section 2.1), we hypothesized that the putative inversion(s) are primarily related to differences between populations east and west of the Appalachian Mountains. In this case, we predicted large  $F_{ST}$  values between the Z chromosome of birds west of the Appalachians and those in the east, but not between the western populations. Indeed, this is the pattern we observed (Figure 5a). There was much higher  $F_{ST}$  on the Z chromosome than the autosomes when we compared birds from west of the main Appalachian Mountain chain (KS, KY, MI, NY, ON and QC) to those

east of the chain (NB, PA; 'East vs. West' in Figure 5a,b). Manhattan plots between these east and west populations suggested a putative inversion around 33–63 Mb on the Z chromosome (Figure S8) similar to the pool-seq samples (Figure 3). Admixture analysis also revealed evidence for more population structure on the Z chromosome than on the autosomes (Figure 5b), particularly between the populations east and west of the Appalachian Mountains. For the autosomes, the admixture cross-validation (CV) error was lowest for one population (CV=0.728, 0.792 and 0.857 for 1, 2 and 3 populations, respectively), whereas for the Z chromosome, the CV error was lowest for two populations (CV=0.760, 0.710 and 0.770 for 1, 2 and 3 populations, respectively). Furthermore, when assuming that there are two ( $K=2$ ) or three ( $K=3$ ) different populations in the east, there are fewer individuals showing mixed ancestry assignments for the Z chromosome than the autosomes (Figure 5b). Intermediate populations (i.e. NY, ON, QC) that are west of the main Appalachian Mountain chain, but typically considered part of the eastern migratory flyway showed

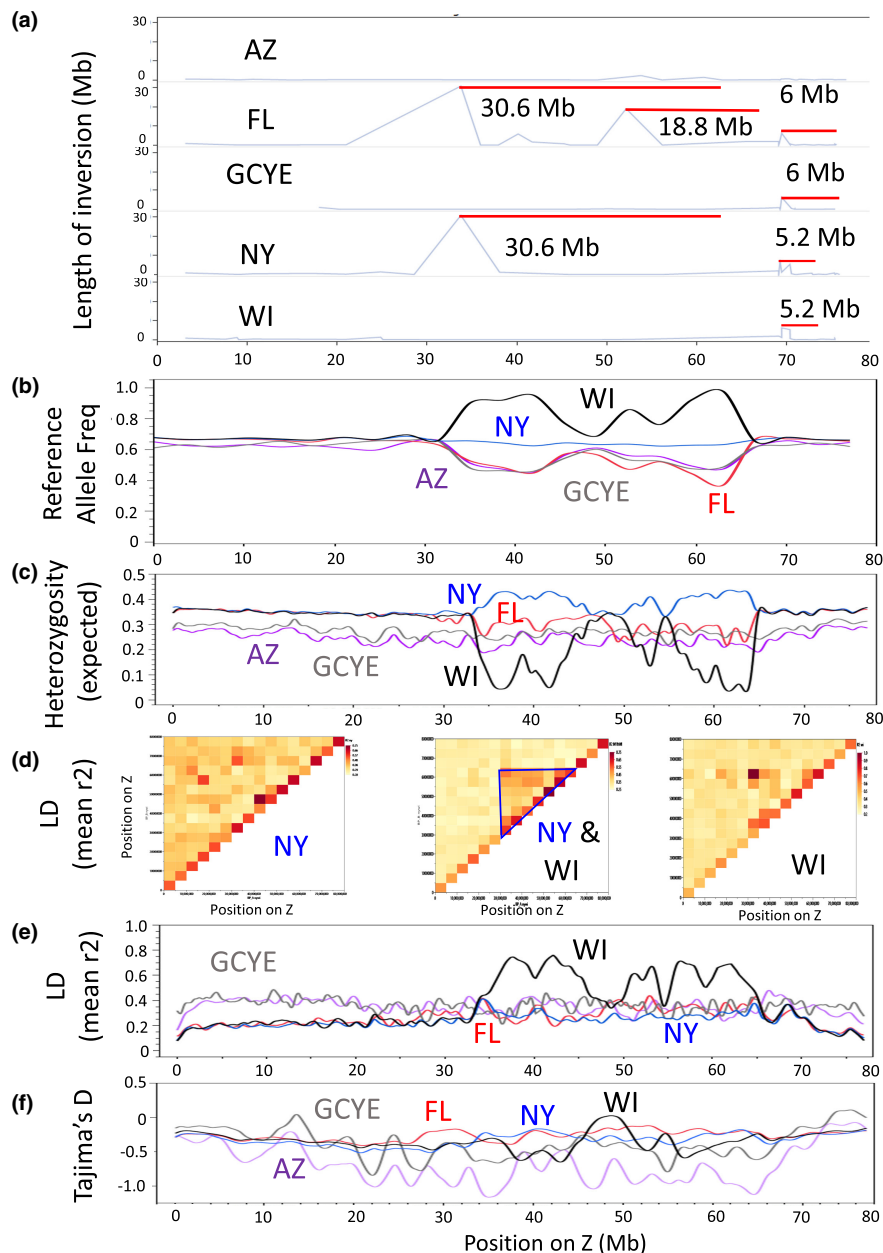


**FIGURE 4** Putative inversions identified by LUMPY that were at least 5 Mb long on the Z chromosome of pooled samples from each study area (a). Panel (a) shows the location of a large inversion 30.6 Mb long (starting at 33.8 Mb) in FL and NY, a second one in FL 18.8 Mb long (starting at 52.1 Mb) and a third 5.2 to 6 Mb long in all the populations except AZ (starting at ~70 Mb). The peaks in the graph indicate the length of the inversion, and the red horizontal bars indicate the length along the x-axis. The breakpoints identified in panel (a) coincided with changes in frequency of the reference allele (b) heterozygosity (c), linkage disequilibrium (d, e) and Tajima's D (f). Panel (d) shows heatmaps of linkage disequilibrium between (centre panel) and within the NY (left panel) and WI (right panel) populations on the Z chromosome analysed using PLINK with ddRAD data ( $n=4284$  SNPs found in all three comparisons). Note the high LD (red colour) in the region of the putative inversion in the centre (NY and WI) comparison (highlighted with a blue triangle), which is less evident in the single population analysis. High correlations (red blocks) along the diagonal in each panel indicate the relatively high correlations between adjacent SNPs. Linkage disequilibrium in panel (e) was analysed using LD with pool-seq data. [Colour figure can be viewed at [wileyonlinelibrary.com](https://onlinelibrary.wiley.com)]

more mixed ancestry, which may indicate more gene flow in this region (see [Figure S1](#) for a map of likely migration routes).

### 3.5 | Differences in morphology between populations were most strongly related to the Z inversion

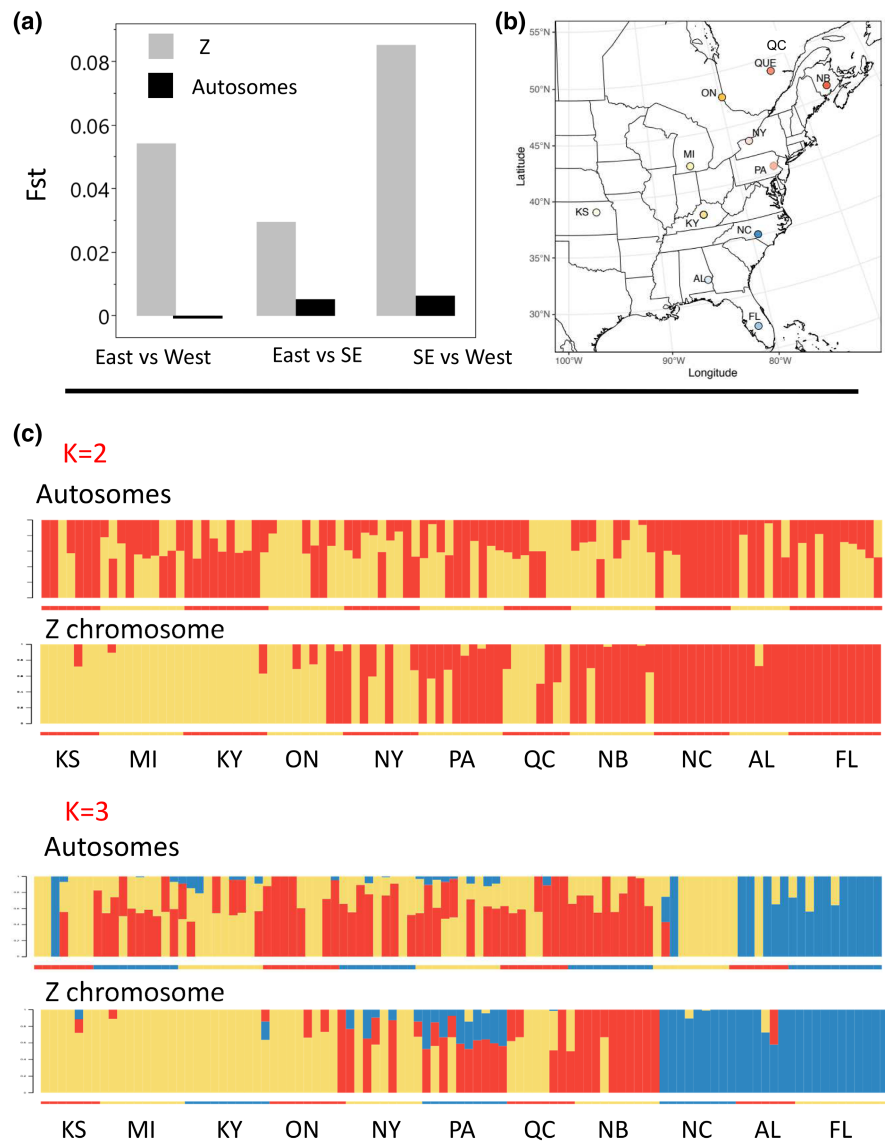
To test whether differences in plumage and ornament size were related more strongly to putative inversions on the Z chromosome than the autosomes, we estimated correlations between SNPs and principal components related to population and ornament size differences in pcAdapt. Here, we focused on the largest putative inversion on the Z chromosome (at 33.8 to 64.4 Mb, [Figure 4a](#)) and compared it to the rest of the Z and the autosomes. If SNPs on the

Z inversion were more closely related to plumage differences than SNPs on the autosomes, then we expected to see stronger correlations on the Z inversion than autosomes.

We began with a PCA of different subspecies of common yellowthroats using the pooled samples from AZ, FL, NY and WI ([Figure 6a](#)). Using 5.23M autosomal SNPs, the PCA showed separation of the AZ (large bib) population from the eastern populations along PC1, and separation of the eastern populations along PC2. The Z chromosome PCA followed a similar pattern. The correlations between genomic variation and these PC axes (from PCAdapt) were stronger for the Z inversion than the rest of the Z chromosome or autosomes for both PC 1 and 2 (all significantly different with Tukey's tests; [Figure 6b](#)).

A similar pattern of divergence was also evident in a comparison of different species and sexes (i.e. when we added grey-crowned

**FIGURE 5** Genomic divergence ( $F_{ST}$ ) was greater on the Z chromosome than the autosomes between populations of common yellowthroats (a). Data are from 100 individuals sequenced at low coverage across their genomes as part of the Bird Genoscape Project ([www.birdgenoscape.org](http://www.birdgenoscape.org)). Panel (b) shows a map of the sample locations. For the analysis in panel (a), locations were coded as west (Kansas, KS; Kentucky, KY; Michigan, MI; New York, NY; Ontario, ON; Quebec, QC) and east of the Appalachian Mountains (New Brunswick, NB; Pennsylvania, PA), or southeast (Alabama, AL; North Carolina, NC; Florida, FL). Panel (c) shows ADMIXTURE plots ( $K=2$  top,  $K=3$  bottom) for these populations based on SNPs (thinned to 1 per 1000) on the autosomes (top) or the Z chromosome (bottom). [Colour figure can be viewed at [wileyonlinelibrary.com](http://wileyonlinelibrary.com)]



yellowthroat and female common yellowthroats from WI to the analysis; [Figure 6c](#)). In this PCA, AZ was separate from the eastern populations again, but on PC2. The addition of grey-crowned yellowthroats (GCYE) had the greatest effect, because it was an outlier on PC1. FL, NY and WI (including females) pools all clustered closer together (on both PC1 and 2). Again, the PC differences were stronger based on SNPs in the Z inversion than the rest of the Z chromosome or the autosomes ([Figure 6d](#)).

Lastly, we performed a GWAS (with GEMMA) examining correlations between morphology (PC1) and SNPs using only the NY and WI populations to reduce the influence of geographic variation, since these are populations of the same subspecies. These data came from ddRAD sequences of individual males for which we also had morphological data at the individual level, in contrast to the pool-seq results. As above, we found that most of the strong associations between morphology and SNPs were found on the Z inversion and not on the autosomes or the rest of the Z chromosome ([Figure 6e](#)). Only two SNPs were significant at a threshold of  $-\log_{10}(p) > 7$ , and they were both on the inversion. There were also relatively more outlier (top

1%) SNPs on the Z inversion (22% were outliers, 15/68 SNPs total), than on the Z chromosome outside the inversion (1.9%, 4/210 total) or on the autosomes (0.6%, 24/3847; [Figure 6e](#)). Overall, 7.4% of the variance in morphology was explained by SNPs on the Z inversion, 5.8% was explained by SNPs on the rest of the Z chromosome, and each autosome explained an average of 1.8% (95 CI: 1.27%–2.33%,  $n=31$  main chromosomes) of the variation in morphology (61% overall for the autosomes).

### 3.6 | Differences in morphology within populations were associated with widespread genes

In contrast to the GWAS results with both NY and WI together ([Figure 6e](#)), when we conducted the GWAS on each population separately, the top 1% of correlations were spread throughout the genome and not clustered in the Z inversion (NY is shown in [Figure 6f](#)). For example, in the NY population, 0.5% of the variance in morphology was explained by SNPs on the inversion, 2.6% was explained by

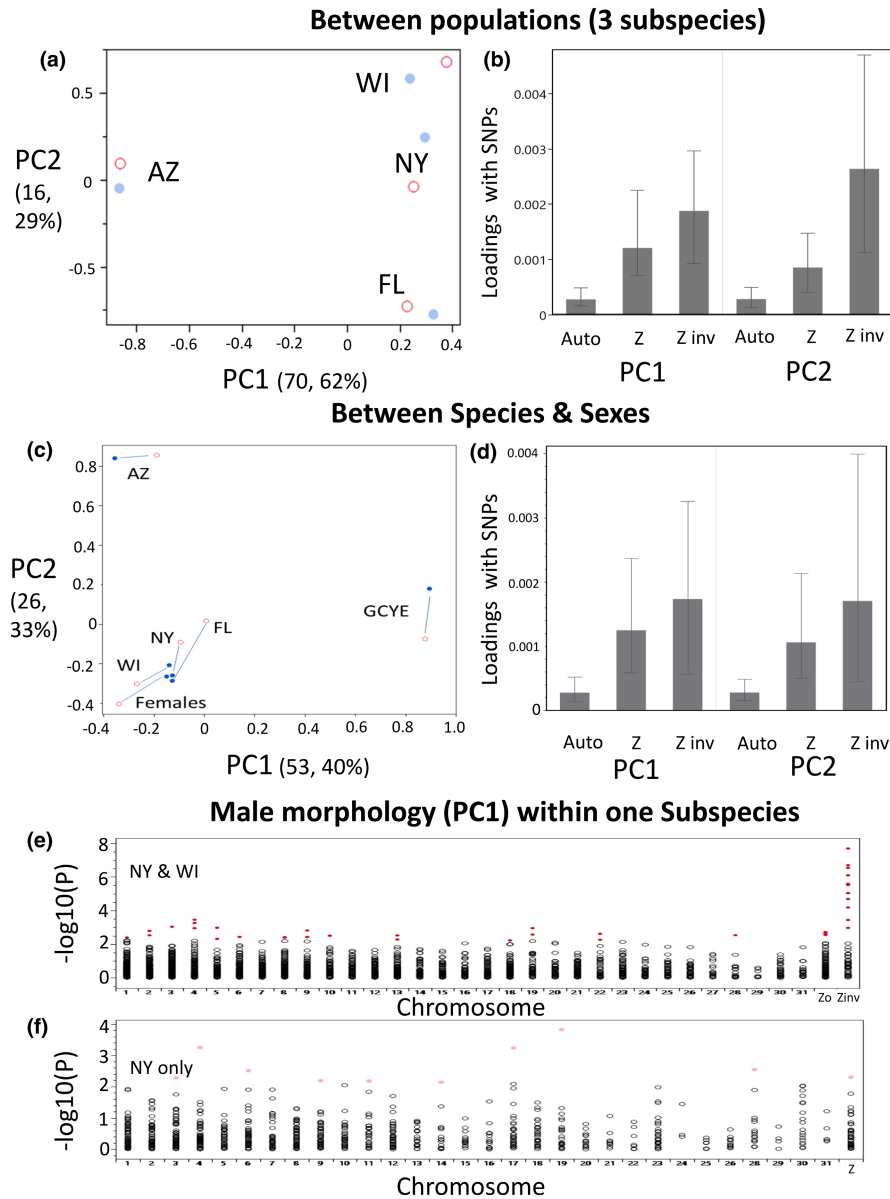


**FIGURE 6** Principal component analysis (PCA) of single-nucleotide polymorphisms (SNPs) from pooled DNA samples in four populations of common yellowthroats analysed with *pcadapt*. Autosomes (red circles;  $N=5.22M$  SNPs) and the Z chromosome (blue;  $N=220,925$  SNPs) are shown together for illustrative purposes, but they were analysed in separate PCAs, so they are not directly comparable. Variance explained (%) for each PC axis is indicated in parentheses for autosomes and Z, respectively. Panel (a) compares populations of three subspecies (*G. t. trichas* from NY and WI; *G. t. ignota*, from FL and *G. t. chryseola* from AZ). Panels on the right (b, d) indicate that there are stronger correlations (PCA loadings) between PC scores (representing population or morphological differences) and individual SNPs for the inversion on the Z chromosome than the rest of the Z or the autosomes. Shown are the median and interquartile range of correlations (loadings) between PC scores (for PC axes 1 & 2 separately) and individual SNPs. PC loadings in panels (b) and (d) between the Z inversion, the rest of the Z and the autosomes were all significantly different with Tukey's tests ( $p < .001$ ). Panels (c) and (d) show the PCA for the same four populations (AZ, FL, NY and WI), as well as the grey-crowned yellowthroat (GCYE) and females from WI, illustrating differences between species and sexes. In these panels blue lines simply connect the same pools for the Z and autosomes for illustrative purposes, but autosomes (red circles) should be interpreted separately from the Z (blue circles). The bottom two panels (e, f) show Manhattan plots for the significance ( $-\log_{10}(p)$ ) of correlations between morphology (PC1) and SNPs across the genome (chromosomes 1–31 and the Z chromosome; Zo indicates the Z outside the inversion and Zinv indicates the Z inside the inversion). Red dots are the top 1% of  $p$ -values. Top panel (e) shows the results from an analysis that combined data from NY and WI, while the bottom panel (f) shows the same analyses with just the NY data. All analyses were from a linear mixed model in GEMMA using ddRAD data from 36 males in NY and 46 males in WI. [Colour figure can be viewed at [wileyonlinelibrary.com](http://wileyonlinelibrary.com)]

SNPs on the rest of the Z chromosome and each autosome explained an average of 1.4% (95 CI: 1.03%–1.84%,  $n=31$  main chromosomes) of the variation in morphology (43% overall for the autosomes). In

this analysis, we used the same PC1 morphology scores for NY individuals as used in the analysis of both NY and WI to eliminate any variation due to different morphological scores (Figure 6e); however,

we also found that the top correlations were spread throughout the genome when PC1 was calculated separately for NY (or WI). Also note that there was no influence of geographic variation in this analysis because each population was analysed separately, and hence, the region with the inversion did not produce any large differences in allele frequencies as found in the between-population analysis.

A similar change in results occurred when we switched from between to within-population comparisons of selection (using SelEstim; Figure S7). In our previous comparison of selection between different populations and subspecies, selection was primarily concentrated on the Z inversion (Figure S7a,b). However, in a comparison of NY individuals with relatively large and small bibs (top and bottom 25th percentiles of size), selection (mean  $\pm$  SE KLD values) did not differ between inside ( $6.73e-3 \pm 2.61e-5$ ) and outside ( $6.68e-3 \pm 1.80e-5$ ) the inversion ( $t=1.77$ ,  $df=17,285$ ,  $p=.07$ ) and the proportion of outliers (top 1%) also did not differ between inside the putative inversion (1.03%, 91/8805) and outside of it (0.98%, 178/18,074, Fisher's exact test  $p=.70$ ; Figure S7c). This pattern extended to other within-population comparisons of ornament size (large and small groups) using the pool-seq data (Figure S9). Thus, the inversion was mainly associated with size and colour differences (PC1) between populations (Figure 6e), but within populations, the same size differences (PC1; Figure 6f), as well as size differences in the sexually selected ornaments (Figure S7c), were associated with polymorphisms spread across the genome.

### 3.7 | Functional annotation of genes on the Z chromosome and its inversion

We investigated the function of genes on the Z chromosome to determine whether they might help to explain the differences in morphology and mate choice between populations. Among the 711 annotated genes on the Z (i.e., including non-outliers), there were seven melanin-related and seven carotenoid-related genes and, of these, two (ALDH1A1 and PCSK5) melanin and four carotenoid (ABCA1, LPL, RBP4 and SLC27A6) genes were on the large Z inversion (from 33.8 to 64.4 Mb; Supporting data Table S1). Another melanin gene (FBN2) was in the smaller (5.2–6 Mb) Z inversion starting at 70 Mb (Figure 4), and an important melanogenesis gene (TYPR1, tyrosinase-related protein 1, at 30.31–30.32 Mb) was about 3 Mb from the large Z inversion.

There were 257 genes within the Z inversion that were also in outlier  $F_{ST}$  windows between populations (Supporting data Table S2). Five genes related to vision were in these outlier windows, including NTRK2, RORB, RPGRIP1L and TOPORS, which are involved in rod cell development (g:profiler enriched gene ontology term; Adjusted  $p=.005$ ), and PDE6B, which is an important gene in the phototransduction pathway (Lagman et al., 2016). The Z inversion also contained two (non-melanogenesis) genes linked to mask size in WI and two linked to bib size in WI in our previous analyses (Sly et al., 2022). Of these, MOB Kinase Activator 3B (MOB3B) is notable as part of the hippo signalling pathway, which regulates organ size and is involved

in feather growth (Sello et al., 2019; Yang et al., 2018), providing a potential link between the inversion and mask size differences between NY and WI.

## 4 | DISCUSSION

An increasing number of studies suggest that large structural variants in the genome, such as inversions and duplications (e.g. copy number variation), are important in producing population structure and local adaptation to the environment (Wellenreuther & Bernatchez, 2018). However, relatively few studies have linked large structural variants to phenotypic traits that are known to play a role in sexual selection and may influence reproductive isolation. Here, we found that a large portion (40%, 31/77 Mb) of the Z chromosome of the common yellowthroat contains putative inversion(s), and variants in that region are associated with more of the male phenotypic differences (in size and plumage) between populations than variants on the rest of the Z chromosome or the autosomes. In the widespread eastern subspecies, *G.t.trichas*, the Z inversions appear to differ primarily east and west of the Appalachian Mountains, providing evidence of cryptic population structure. Furthermore, in at least two of these populations east (NY) and west (WI) of the Appalachians there are also differences in female mating preferences for different male ornaments (black facial mask or yellow breast; Dunn et al., 2008; Sly et al., 2022). Thus, the structural variants on the Z chromosome could contribute to reducing gene flow between the east and west populations (in addition to migratory differences), which, in turn, could help to maintain different patterns of sexual selection, even within the same subspecies. It is also important to note that within populations all or most individuals appeared to share the same inversion type, and, in this case, morphological (ornament size) variation was related to SNPs spread more broadly across the genome, as we had reported previously in transcriptome and pool-seq analyses of ornament size within the NY and WI populations (Sly et al., 2022). Thus, selection on morphology (and sexually selected ornaments, in particular) appears to vary with the genomic architecture (e.g. inversions) of a population and the level of analysis (within or between populations). This has important implications for interpreting studies of the genomic basis of sexually selected ornaments because the level of analysis may be related to different aspects of sexual selection. For example, between-population analyses may reveal genes related to mate choice for locally adapted genes (e.g. avoidance of outbreeding or hybridization); in common, yellowthroats this may include different ornament preferences (mask or bib) in different populations. In contrast, within-population analyses may reveal genes related to female choice of high-quality mates (e.g. the size of the bib in NY or mask in WI).

Sexual selection has often been considered a driver of diversification and speciation because female choice can lead to divergence in the colour and size of male ornaments between different populations, and ultimately reproductive isolation. To date, genomic studies have often focused on the regulation of pigmentation genes that can

produce large, discrete differences in patches used in species recognition, which could, in turn, lead to reproductive isolation. Several genomic studies in birds (Campagna et al., 2022; Toews et al., 2016) and fish (Hench et al., 2019) have found divergence between closely related species can be limited to just a few pigmentation genes that affect colour patterns, with little differentiation elsewhere in the genome. However, in other studied regions of differentiation between species are scattered more widely across the genome (e.g. Feulner et al., 2015; Meier et al., 2018). In common yellowthroats (this study) and hybridizing orioles (Walsh et al., 2023), divergence in plumage between populations and species, respectively, was primarily associated with large (>30Mb) inversions on the Z chromosome. In the orioles 90% of the SNPs related to plumage were on the Z inversion, while in yellowthroats the percentage was much lower (22% for PC1 differences between populations of the same subspecies; NY vs. WI). This difference may reflect a presumably longer divergence time between species (in orioles) than subspecies (yellowthroats). Walsh et al. (2023) attributed the large differences between oriole species ( $F_{ST}=0.19$ ) to a deep divergence time (350k years), which has provided time for more polymorphisms to accumulate. In contrast, common yellowthroats east and west of the Appalachian Mountains are still considered the same subspecies and probably have considerable gene flow between them ( $F_{ST}$  between NY and WI=0.073 and 0.005 for Z and autosomes, respectively), so the putative Z inversion may be relatively recent and may not have allowed the build-up of large  $F_{ST}$  differences as seen in orioles.

Inversions are expected to be favoured by selection when they contain alleles that promote local adaptation as well as reproductive isolation (Felsenstein, 1981; Schaal et al., 2022). In this respect, it is interesting that, in addition to the genes related to male phenotype, we also found several genes in the inversion that are related to vision. This suggests that genes related to both male phenotype and female mate preferences are on the same inversion. Female preference differs between two of the common yellowthroat populations (WI and NY) east and west of the Appalachian Mountains. In WI females prefer males with larger masks and these males have greater social and extra-pair mating success, but females prefer males with larger bills in NY and these males are also more successful in terms of mating success (Dunn et al., 2008; Freeman-Gallant et al., 2010). Within the Z inversion, we found five genes related to vision, including one of the phosphodiesterase genes, PDGE6B, which plays a critical role in the phototransduction cascade and is associated with several retinal diseases in humans and reduced visual acuity in domesticated chickens relative to their wild ancestor, the red junglefowl (Lagman et al., 2016; Wang et al., 2016). These vision-related genes could potentially be involved in differences in mate choice at the population level; however, further study is needed of their specific role in vision in different populations.

Genes for both male plumage and vision were also found in inversions in the orioles studied by Walsh et al. (2023) and crows in Europe (Poelstra et al., 2014). The Z inversions in common yellowthroats (33.8–64.4 Mb) and orioles (1.7–45.4 Mb, Walsh et al., 2023) overlap for 12 Mb on the Z (including the five vision-related genes

mentioned above), so some of the same vision and plumage related genes may be involved in divergence of different species or subspecies. In crows there were several genes related to melanogenesis and one gene (RGS9) related to vision on an inversion on chromosome 18 (Poelstra et al., 2014). Several other studies of fish (Hench et al., 2019) and insects (Merrill et al., 2019; Rossi et al., 2024) have also found similar linkages between genes for male traits and female preference, but they do not appear to be associated with inversions. Thus, there appear to be several mechanisms for how trait and preference genes become associated.

As in previous studies, we found pigmentation genes were associated with the top divergence peaks in all population comparisons of yellowthroats, but they were not overrepresented in those peaks. Melanogenesis, which controls the expression of black patches in a variety of taxa, is regulated by several distinct signalling pathways (Ducrest et al., 2008; Serre et al., 2018). We found divergent genes in these signalling pathways, including KIT, MC1R/Agouti and WNT in various comparisons of subspecies. Thus, melanin patches in yellowthroat plumage may be regulated by a diverse set of signalling genes, in contrast to some previous studies that have found repeated evolution of the same gene (e.g. Agouti signalling protein [ASIP]) regulating melanin differences among closely related populations or species (Baiz, Kramer, et al., 2020; Baiz, Wood, et al., 2020; Price-Waldman & Stoddard, 2021). We also found a few examples of carotenoid-related genes that were divergent across yellowthroat populations and may be related to differences in the yellow on the throat. For example, the scavenger receptor SCARF2 was divergent between common and grey-crowned yellowthroats. The scavenger receptor SCARF2 binds and transports lipoprotein complexes involved in carotenoid transport, and this gene has been previously linked to carotenoid pigmentation in birds (Brelsford et al., 2017). In yellowthroats, the main carotenoid pigment is dietary lutein, which is deposited into the plumage with little enzymatic modification (McGraw et al., 2003). Therefore, it is not surprising that we did not find divergence in enzymes that metabolize carotenoids such as CYP2J19 (Lopes et al., 2016) and BCO2 (Gazda et al., 2020) which have been linked to carotenoid colour shifts in birds that have different types of carotenoids in their plumage. Instead, we found genes related to either carotenoid transport (SCARF2; Brelsford et al., 2017) or to the absorption of dietary carotenoids (ISX in the comparison of WI and NY; Bohn et al., 2017).

## 5 | CONCLUSIONS

Our results provide evidence that a large inversion on the Z chromosome (40% of the Z chromosome) is related to differences between populations in male size and colour, including their sexually selected ornaments. These ornaments are also associated with differences in female mate choice between closely related populations and, hence, potentially to population divergence. The inversions on the Z chromosome vary geographically, particularly east and west of the Appalachian Mountains, which is within the range of one subspecies

(*G. t. trichas*). This subspecies diverged within the last 1 M years based on mitochondrial sequences (Escalante et al., 2009) and possibly more recently following range expansion after the last Pleistocene glaciation (Boulet & Gibbs, 2006; Lovette, 2005). A more recent divergence is consistent with theory that larger inversions should form early in the speciation process, partly because they prevent recombination from breaking up adaptive allele combinations (Schaal et al., 2022). In contrast to the between-population comparisons, within-population comparisons revealed that variation in male size and colour was associated with SNPs spread across the genome, as we found previously (Sly et al., 2022). Within populations, all or most of the individuals presumably shared the same inversion type, so it was only when we performed between-population comparisons in this study that the importance of the putative Z inversion became apparent. Thus, ornament-related genes on the Z chromosome are important in comparisons of different populations, but they are less important for explaining variation within populations which may be related to local selective forces, such as mate choice for high-quality mates. This has important implications for interpreting studies of the genomic basis of sexually selected ornaments because different parts of the genome (e.g. inversions) may be related to different aspects of sexual selection (e.g. avoidance of outbreeding or choice of high-quality mates).

#### AUTHOR CONTRIBUTIONS

P.O.D., L.A.W. and C.R.F.-G. designed the study. All authors contributed to fieldwork or provided data or genomic resources. P.O.D. and N.D.S. analysed the data and wrote the initial draft of the manuscript. All authors contributed to the final version.

#### ACKNOWLEDGEMENTS

We thank M. Chamberlain, K. Savides, R. Schneider, B. Shortreed, C. Taff and the staff of the University of Wisconsin–Milwaukee (UWM) Field Station for field assistance in the United States and W. Martinez, R. Cal, and S. Reneau for field assistance at Runaway Creek Nature Preserve in Belize, the Vertebrate Genome Project for construction of the reference genome, the National Center for Genome Analysis Support at Indiana University and the UWM High Performance Computing Service for computing time and consulting. We thank Jess McLaughlin for the yellowthroat illustrations and the editor and reviewers for helpful comments. For logistical help and assistance with permits, we thank S. Wilcox (Appleton-Whittell Research Ranch), C. Kondrat-Smith (AZ Game and Fish Department Sci Permit SP653950), M. Lawrence (Patagonia Sonoita Creek Preserve), M. Radke (BLM San Pedro Riparian and Las Cienegas National Conservation Area) in Arizona, S. Corilla (Belize Forest Department) and K. Hartwell (Runaway Creek Nature Reserve) in Belize, R. Bowman (Archbold Biological Station) in Florida and N. Rivers (Sci Coll Permit SCPN-19-60) in Wisconsin. We thank Danny Bystrak and the USGS Patuxent Wildlife Research Center for band recovery data of common yellowthroats. Birds were banded and samples imported under permits: Dunn Banding permit 22385, AZ Scientific Permit SP653950, FL Scientific Collecting Permit WB07219, WI Scientific

Collecting Permit SCPN-19-60, USDA/APHIS veterinary permit for importation 126881, USFWS Import licence 54562B, Belize Forest Dept Permits (Sci research: FD/WL/1/19; export: FD/WL/7/19) and Belize Agricultural Health Authority (QWC1939/05/P64).

#### FUNDING INFORMATION

This work was supported by grants from the National Science Foundation (IOS-1601093 to L.A.W. and A.E.H.; IOS-1749044 to P.O.D. and L.A.W.; IOS-1749052 to C.R.F.-G.; and DEB-1942313 to K.C.R.), National Geographic Society (WW-202R-17 to K.C.R.) and the National Science Centre in Poland (2015/19/D/NZ8/01310 to P.M.).

#### CONFLICT OF INTEREST STATEMENT

The authors declare no conflict of interest.

#### DATA AVAILABILITY STATEMENT

Sequencing reads from pooled whole-genome analyses have been deposited in the Sequence Read Archive (<https://www.ncbi.nlm.nih.gov/sra>) under Bioproject PRJNA734331. All other study data are on Dryad (Dunn et al., 2023; <https://doi.org/10.5061/dryad.g1jwstqxd>) or included in the article or Appendix S1.

#### ORCID

Peter O. Dunn  <https://orcid.org/0000-0002-7450-4194>

Linda A. Whittingham  <https://orcid.org/0000-0002-7818-6963>

#### REFERENCES

- Alexander, D. H., Novembre, J., & Lange, K. (2009). Fast model-based estimation of ancestry in unrelated individuals. *Genome Research*, 19(9), 1655–1664.
- Baiz, M. D., Kramer, G. R., Streby, H. M., Taylor, S. A., Lovette, I. J., & Toews, D. P. L. (2020). Genomic and plumage variation in *Vermivora* hybrids. *Auk*, 137, ukaa027. <https://doi.org/10.1093/auk/ukaa027>
- Baiz, M. D., Wood, A. W., Brelsford, A., Lovette, I. J., & Toews, D. P. L. (2020). Pigmentation genes show evidence of repeated divergence and multiple bouts of introgression in *Setophaga* warblers. *Current Biology*, 31, 643–649. <https://doi.org/10.1016/j.cub.2020.1010.1094>
- Barth, J. M. I., Villegas-Ríos, D., Freitas, C., Moland, E., Star, B., André, C., Knutsen, H., Bradbury, I., Dierking, J., Petereit, C., Righton, D., Metcalfe, J., Jakobsen, K. S., Olsen, E. M., & Jentoft, S. (2019). Disentangling structural genomic and behavioural barriers in a sea of connectivity. *Molecular Ecology*, 28(6), 1394–1411. <https://doi.org/10.1111/mec.15010>
- Bohn, T., Desmarchelier, C., Dragsted, L. O., Nielsen, C. S., Stahl, W., Rühl, R., Keijer, J., & Borel, P. (2017). Host-related factors explaining interindividual variability of carotenoid bioavailability and tissue concentrations in humans. *Molecular Nutrition & Food Research*, 61(6), 1600685. <https://doi.org/10.1002/mnfr.201600685>
- Bolger, A. M., Lohse, M., & Usadel, B. (2014). Trimmomatic: A flexible trimmer for Illumina sequence data. *Bioinformatics*, 30(15), 2114–2120. <https://doi.org/10.1093/bioinformatics/btu170>
- Boulet, M., & Gibbs, H. L. (2006). Lineage origin and expansion of a Neotropical migrant songbird after recent glaciation events. *Molecular Ecology*, 15(9), 2505–2525. <https://doi.org/10.1111/j.1365-294X.2006.02956.x>
- Brelsford, A., Toews, D. P. L., & Irwin, D. E. (2017). Admixture mapping in a hybrid zone reveals loci associated with avian feather coloration. *Proceedings of the Royal Society B: Biological Sciences*, 284(1866), 20171106. <https://doi.org/10.1098/rspb.2017.1106>

- Campagna, L., Mo, Z., Siepel, A., & Uy, J. A. C. (2022). Selective sweeps on different pigmentation genes mediate convergent evolution of Island melanism in two incipient bird species. *PLoS Genetics*, 18(11), e1010474. <https://doi.org/10.1371/journal.pgen.1010474>
- Catchen, J., Hohenlohe, P. A., Bassham, S., Amores, A., & Cresko, W. A. (2013). Stacks: An analysis tool set for population genomics. *Molecular Ecology*, 22(11), 3124–3140. <https://doi.org/10.1111/mec.12354>
- Charlesworth, B., Coyne, J. A., & Barton, N. H. (1987). The relative rates of evolution of sex chromosomes and autosomes. *The American Naturalist*, 130(1), 113–146. <https://doi.org/10.1086/284701>
- Cruikshank, T. E., & Hahn, M. W. (2014). Reanalysis suggests that genomic islands of speciation are due to reduced diversity, not reduced gene flow. *Molecular Ecology*, 23(13), 3133–3157. <https://doi.org/10.1111/mec.12796>
- Danecek, P., Auton, A., Abecasis, G., Albers, C. A., Banks, E., DePristo, M. A., Handsaker, R. E., Lunter, G., Marth, G. T., Sherry, S. T., McVean, G., Durbin, R., & Genomes Project Analysis Group. (2011). The variant call format and VCFtools. *Bioinformatics*, 27(15), 2156–2158.
- Ducrest, A.-L., Keller, L., & Roulin, A. (2008). Pleiotropy in the melanocortin system, coloration and behavioural syndromes. *Trends in Ecology & Evolution*, 23(9), 502–510.
- Dunn, P. O., Sly, N. D., Freeman-Gallant, R., Henschen, A., Bossu, C. M., Ruegg, A. R., Minias, P., & Whittingham, L. A. (2023). *Data from: Sexually-selected differences in warbler plumage are related to a putative inversion on the Z chromosome. Dryad Data.* <https://doi.org/10.5061/dryad.g1jwstqxd>
- Dunn, P. O., Whittingham, L. A., Freeman-Gallant, C. R., & DeCoste, J. (2008). Geographic variation in the function of ornaments in the common yellowthroat *Geothlypis trichas*. *Journal of Avian Biology*, 39(1), 66–72. <https://doi.org/10.1111/j.2008.0908-8857.04113.x>
- Escalante, P., Márquez-Valdelamar, L., Torre, P., de la Torre, P., Lacleste, J. P., & Klicka, J. (2009). Evolutionary history of a prominent north American warbler clade: The *Oporornis-Geothlypis* complex. *Molecular Phylogenetics and Evolution*, 53(3), 668–678. <https://doi.org/10.1016/j.ympev.2009.07.014>
- Feder, A. F., Petrov, D. A., & Bergland, A. O. (2012). LDx: Estimation of linkage disequilibrium from high-throughput pooled resequencing data. *PLoS One*, 7(11), e48588. <https://doi.org/10.1371/journal.pone.0048588>
- Felsenstein, J. (1981). Skepticism towards Santa Rosalia, or why are there so few kinds of animals? *Evolution*, 35(1), 124–138. <https://doi.org/10.2307/2407946>
- Feulner, P. G., Chain, F. J., Panchal, M., Huang, Y., Eizaguirre, C., Kalbe, M., Lenz, T. L., Samonte, I. E., Stoll, M., Bornberg-Bauer, E., Reusch, T. B., & Milinski, M. (2015). Genomics of divergence along a continuum of parapatric population differentiation. *PLoS Genetics*, 11(2), e1004966. <https://doi.org/10.1371/journal.pgen.1004966>
- Freeman-Gallant, C. R., Taff, C. C., Morin, D. F., Dunn, P. O., Whittingham, L. A., & Tsang, S. M. (2010). Sexual selection, multiple male ornaments, and age- and condition-dependent signaling in the common yellowthroat. *Evolution*, 64(4), 1007–1017. <https://doi.org/10.1111/j.1558-5646.2009.00873.x>
- Gautier, M. (2015). Genome-wide scan for adaptive divergence and association with population-specific covariates. *Genetics*, 201(4), 1555–1579. <https://doi.org/10.1534/genetics.115.181453>
- Gautier, M., Vitalis, R., Flori, L., & Estoup, A. (2022). F-statistics estimation and admixture graph construction with Pool-Seq or allele count data using the R package poolstat. *Molecular Ecology Resources*, 22(4), 1394–1416. <https://doi.org/10.1111/1755-0998.13557>
- Gazda, M. A., Araújo, P. M., Lopes, R. J., Toomey, M. B., Andrade, P., Afonso, S., Marques, C., Nunes, L., Pereira, P., Trigo, S., Hill, G. E., Corbo, J. C., & Carneiro, M. (2020). A genetic mechanism for sexual dichromatism in birds. *Science*, 368(6496), 1270–1274. <https://doi.org/10.1126/science.aba0803>
- Guzy, M. J., & Ritchison, G. (1999). Common yellowthroat. In A. Poole & F. Gill (Eds.), *The birds of North America* Vol. 448 (pp. 1–23). Cornell Laboratory of Ornithology and The Academy of Natural Sciences.
- Hench, K., Vargas, M., Höppner, M. P., McMillan, W. O., & Puebla, O. (2019). Inter-chromosomal coupling between vision and pigmentation genes during genomic divergence. *Nature Ecology & Evolution*, 3(4), 657–667. <https://doi.org/10.1038/s41559-019-0814-5>
- Hooper, D. M., Griffith, S. C., & Price, T. D. (2019). Sex chromosome inversions enforce reproductive isolation across an avian hybrid zone. *Molecular Ecology*, 28(6), 1246–1262. <https://doi.org/10.1111/mec.14874>
- Hooper, D. M., & Price, T. D. (2017). Chromosomal inversion differences correlate with range overlap in passerine birds. *Nature Ecology & Evolution*, 1(10), 1526–1534. <https://doi.org/10.1038/s41559-017-0284-6>
- Howe, K., Chow, W., Collins, J., Pelan, S., Pointon, D.-L., Sims, Y., Torrance, J., Tracey, A., & Wood, J. (2021). Significantly improving the quality of genome assemblies through curation. *GigaScience*, 10(1), g1aa153. <https://doi.org/10.1093/gigascience/g1aa153>
- Irwin, D. E. (2018). Sex chromosomes and speciation in birds and other ZW systems. *Molecular Ecology*, 27, 3831–3851. <https://doi.org/10.1111/mec.14537>
- Irwin, D. E., Milá, B., Toews, D. P. L., Brelsford, A., Kenyon, H. L., Porter, A. N., Grossen, C., Delmore, K. E., Alcaide, M., & Irwin, J. H. (2018). A comparison of genomic islands of differentiation across three young avian species pairs. *Molecular Ecology*, 27(23), 4839–4855. <https://doi.org/10.1111/mec.14858>
- Jain, C., Rodriguez-R, L. M., Phillippy, A. M., Konstantinidis, K. T., & Aluru, S. (2018). High throughput ANI analysis of 90K prokaryotic genomes reveals clear species boundaries. *Nature Communications*, 9(1), 5114. <https://doi.org/10.1038/s41467-018-07641-9>
- Jay, P., Chouteau, M., Whibley, A., Bastide, H., Parrinello, H., Llaurens, V., & Joron, M. (2021). Mutation load at a mimicry supergene sheds new light on the evolution of inversion polymorphisms. *Nature Genetics*, 53(3), 288–293. <https://doi.org/10.1038/s41588-020-00771-1>
- Jones, F. C., Grabherr, M. G., Chan, Y. F., Russell, P., Mauceli, E., Johnson, J., Swofford, R., Pirun, M., Zody, M. C., White, S., Birney, E., Searle, S., Schmutz, J., Grimwood, J., Dickson, M. C., Myers, R. M., Miller, C. T., Summers, B. R., Knecht, A. K., ... Kingsley, D. M. (2012). The genomic basis of adaptive evolution in threespine sticklebacks. *Nature*, 484(7392), 55–61. <https://doi.org/10.1038/nature10944>
- Knief, U., Bossu, C. M., Saino, N., Hansson, B., Poelstra, J., Vijay, N., Weissensteiner, M., & Wolf, J. B. W. (2019). Epistatic mutations under divergent selection govern phenotypic variation in the crow hybrid zone. *Nature Ecology & Evolution*, 3(4), 570–576. <https://doi.org/10.1038/s41559-019-0847-9>
- Kofler, R., Orozco-terWengel, P., De Maio, N., Pandey, R. V., Nolte, V., Futschik, A., Kosiol, C., & Schlötterer, C. (2011). PoPoolation: A toolbox for population genetic analysis of next generation sequencing data from pooled individuals. *PLoS One*, 6(1), e15925.
- Kofler, R., Pandey, R. V., & Schlötterer, C. (2011). PoPoolation2: Identifying differentiation between populations using sequencing of pooled DNA samples (Pool-Seq). *Bioinformatics*, 27(24), 3435–3436.
- Krueger, F. (2020). TrimGalore, GitHub repository. <https://github.com/FelixKrueger/TrimGalore>
- Kupper, C., Stocks, M., Risse, J. E., Dos Remedios, N., Farrell, L. L., McRae, S. B., Morgan, T. C., Karlionova, N., Pinchuk, P., Verkuil, Y. I., Kitaysky, A. S., Wingfield, J. C., Piersma, T., Zeng, K., Slate, J., Blaxter, M., Lank, D. B., & Burke, T. (2015). A supergene determines highly divergent male reproductive morphs in the ruff. *Nature Genetics*, 48, 79–83. <https://doi.org/10.1038/ng.3443>
- Lagman, D., Franzén, I. E., Eggert, J., Larhammar, D., & Abalo, X. M. (2016). Evolution and expression of the phosphodiesterase 6 genes unveils vertebrate novelty to control photosensitivity. *BMC Evolutionary Biology*, 16(1), 124. <https://doi.org/10.1186/s12862-016-0695-z>

- Lamichhane, S., & Andersson, L. (2019). A comparison of the association between large haplotype blocks under selection and the presence/absence of inversions. *Ecology and Evolution*, 9(8), 4888–4896. <https://doi.org/10.1002/ece3.5094>
- Layer, R. M., Chiang, C., Quinlan, A. R., & Hall, I. M. (2014). LUMPY: A probabilistic framework for structural variant discovery. *Genome Biology*, 15(6), R84. <https://doi.org/10.1186/gb-2014-15-6-r84>
- Li, H., & Durbin, R. (2010). Fast and accurate long-read alignment with burrows-wheeler transform. *Bioinformatics*, 26(5), 589–595. <https://doi.org/10.1093/bioinformatics/btp698>
- Lopes, R. J., Johnson, J. D., Toomey, M. B., Ferreira, M. S., Araujo, P. M., Melo-Ferreira, J., Andersson, L., Hill, G. E., Corbo, J. C., & Carneiro, M. (2016). Genetic basis for red coloration in birds. *Current Biology*, 26(11), 1427–1434. <https://doi.org/10.1016/j.cub.2016.03.076>
- Lovette, I. J. (2005). Glacial cycles and the tempo of avian speciation. *Trends in Ecology & Evolution*, 20(2), 57–59. <https://doi.org/10.1016/j.tree.2004.11.011>
- Lu, C.-W., Huang, S.-T., Cheng, S.-J., Lin, C.-T., Hsu, Y.-C., Yao, C.-T., Dong, F., Hung, C.-M., & Kuo, H.-C. (2023). Genomic architecture underlying morphological and physiological adaptation to high elevation in a songbird. *Molecular Ecology*, 32, 2234–2251. <https://doi.org/10.1111/mec.16875>
- Luu, K., Bazin, E., & Blum, M. G. B. (2017). Pcadapt: An R package to perform genome scans for selection based on principal component analysis. *Molecular Ecology Resources*, 17(1), 67–77. <https://doi.org/10.1111/1755-0998.12592>
- Mahmoud, M., Gobet, N., Cruz-Dávalos, D. I., Mounier, N., Dessimoz, C., & Sedlazeck, F. J. (2019). Structural variant calling: The long and the short of it. *Genome Biology*, 20, 1–14. <https://doi.org/10.1186/s13059-019-1828-7>
- McCallum, Q., Askelson, K., Fogarty, F. F., Natola, L., Nikelski, E., Huang, A., & Irwin, D. (2024). Pronounced differentiation on the Z chromosome and parts of the autosomes in crowned sparrows contrasts with mitochondrial paraphyly: Implications for speciation. *Journal of Evolutionary Biology*, 37(2), 171–188. <https://doi.org/10.1093/jeb/voae004>
- McGraw, K. J., Beebee, M. D., Hill, G. E., & Parker, R. S. (2003). Lutein-based plumage coloration in songbirds is a consequence of selective pigment incorporation into feathers. *Comparative Biochemistry and Physiology. B*, 135(6), 689–696.
- Meier, J. I., Marques, D. A., Wagner, C. E., Excoffier, L., & Seehausen, O. (2018). Genomics of parallel ecological speciation in Lake Victoria cichlids. *Molecular Biology and Evolution*, 35(6), 1489–1506. <https://doi.org/10.1093/molbev/msy051>
- Mendelson, T. C., Martin, M. D., & Flaxman, S. M. (2014). Mutation-order divergence by sexual selection: Diversification of sexual signals in similar environments as a first step in speciation. *Ecology Letters*, 17(9), 1053–1066. <https://doi.org/10.1111/ele.12313>
- Merrill, R. M., Rastas, P., Martin, S. H., Melo, M. C., Barker, S., Davey, J., McMillan, W. O., & Jiggins, C. D. (2019). Genetic dissection of assortative mating behavior. *PLoS Biology*, 17(2), e2005902. <https://doi.org/10.1371/journal.pbio.2005902>
- Nei, M., & Li, W. H. (1979). Mathematical model for studying genetic variation in terms of restriction endonucleases. *Proceedings of the National Academy of Sciences of the United States of America*, 76(10), 5269–5273. <https://doi.org/10.1073/pnas.76.10.5269>
- Peterson, B. K., Weber, J. N., Kay, E. H., Fisher, H. S., & Hoekstra, H. E. (2012). Double digest RADseq: An inexpensive method for *de novo* SNP discovery and genotyping in model and non-model species. *PLoS One*, 7(5), e37135. <https://doi.org/10.1371/journal.pone.0037135>
- Poelstra, J. W., Vijay, N., Bossu, C. M., Lantz, H., Ryll, B., Müller, I., Baglione, V., Unneberg, P., Wikelski, M., Grabherr, M. G., & Wolf, J. B. W. (2014). The genomic landscape underlying phenotypic integrity in the face of gene flow in crows. *Science*, 344(6190), 1410–1414. <https://doi.org/10.1126/science.1253226>
- Price-Waldman, R., & Stoddard, M. C. (2021). Avian coloration genetics: Recent advances and emerging questions. *Journal of Heredity*, 112, 395–416. <https://doi.org/10.1093/jhered/esab015>
- Purcell, S., Neale, B., Todd-Brown, K., Thomas, L., Ferreira, M. A. R., Bender, D., Maller, J., Sklar, P., de Bakker, P. I. W., Daly, M. J., & Sham, P. C. (2007). PLINK: A tool set for whole-genome association and population-based linkage analyses. *The American Journal of Human Genetics*, 81(3), 559–575. <https://doi.org/10.1086/519795>
- Raudvere, U., Kolberg, L., Kuzmin, I., Arak, T., Adler, P., Peterson, H., & Vilo, J. (2019). G:Profiler: A web server for functional enrichment analysis and conversions of gene lists (2019 update). *Nucleic Acids Research*, 47(W1), W191–W198. <https://doi.org/10.1093/nar/gkz369>
- Rhie, A., McCarthy, S. A., Fedrigo, O., Damas, J., Formenti, G., Koren, S., Uliano-Silva, M., Chow, W., Functamman, A., Gedman, G. L., Cantin, L. J., Thibaud-Nissen, F., Haggerty, L., Lee, C., Ko, B. J., Kim, J., Bista, I., Smith, M., Haase, B., ... Diekhans, M. (2020). Towards complete and error-free genome assemblies of all vertebrate species. *bioRxiv*, 2020.2005.2022.110833. <https://doi.org/10.1101/2020.05.22.110833>
- Rossi, M., Hausmann, A. E., Alcamí, P., Moest, M., Roussou, R., Van Belleghem, S. M., Wright, D. S., Kuo, C.-Y., Lozano-Urrego, D., Maulana, A., Melo-Flórez, L., Rueda-Muñoz, G., McMahon, S., Linares, M., Osman, C., McMillan, W. O., Pardo-Díaz, C., Salazar, C., & Merrill, R. M. (2024). Adaptive introgression of a visual preference gene. *Science*, 383(6689), 1368–1373. <https://doi.org/10.1126/science.adj9201>
- Sanchez-Donoso, I., Ravagni, S., Rodríguez-Teijeiro, J. D., Christmas, M. J., Huang, Y., Maldonado-Linares, A., Puigcerver, M., Jiménez-Blasco, I., Andrade, P., Gonçalves, D., Friis, G., Roig, I., Webster, M. T., Leonard, J. A., & Vilà, C. (2021). Massive genome inversion drives coexistence of divergent morphs in common quails. *Current Biology*, 32, 462–469. <https://doi.org/10.1016/j.cub.2021.11.019>
- SAS Institute. 2020. JMP Pro v. 16. Cary, NC.
- Schaal, S. M., Haller, B. C., & Lotterhos, K. E. (2022). Inversion invasions: When the genetic basis of local adaptation is concentrated within inversions in the face of gene flow. *Philosophical Transactions of the Royal Society, B: Biological Sciences*, 377(1856), 20210200. <https://doi.org/10.1098/rstb.2021.0200>
- Schlotterer, C., Tobler, R., Kofler, R., & Nolte, V. (2014). Sequencing pools of individuals - mining genome-wide polymorphism data without big funding. *Nature Reviews Genetics*, 15(11), 749–763. <https://doi.org/10.1038/nrg3803>
- Sello, C. T., Liu, C., Sun, Y., Msuthwana, P., Hu, J., Sui, Y., Chen, S., Zhou, Y., Lu, H., Xu, C., Sun, Y., Liu, J., Li, S., & Yang, W. (2019). *De novo* assembly and comparative transcriptome profiling of *Anser anser* and *Anser cygnoides* geese species' embryonic skin feather follicles. *Genes*, 10(5), 351. <https://doi.org/10.3390/genes10050351>
- Serre, C., Busutil, V., & Botto, J. M. (2018). Intrinsic and extrinsic regulation of human skin melanogenesis and pigmentation. *International Journal of Cosmetic Science*, 40(4), 328–347. <https://doi.org/10.1111/ics.12466>
- Servedio, M. R., & Boughman, J. W. (2017). The role of sexual selection in local adaptation and speciation. *Annual Review of Ecology, Evolution, and Systematics*, 48(1), 85–109. <https://doi.org/10.1146/annurev-ecolsys-110316-022905>
- Sham, P. C., & Purcell, S. M. (2014). Statistical power and significance testing in large-scale genetic studies. *Nature Reviews Genetics*, 15(5), 335–346. <https://doi.org/10.1038/nrg3706>
- Sly, N. D., Freeman-Gallant, C. R., Henschen, A. E., Minias, P., Whittingham, L. A., & Dunn, P. O. (2022). Molecular parallelism in signaling function across different sexually selected ornaments in a warbler. *Proceedings of the National Academy of Sciences of the United States of America*, 119(8), e2120482119. <https://doi.org/10.1073/pnas.2120482119>

- Toews, D. P., Taylor, S. A., Vallender, R., Brelsford, A., Butcher, B. G., Messer, P. W., & Lovette, I. J. (2016). Plumage genes and little else distinguish the genomes of hybridizing warblers. *Current Biology*, 26(17), 2313–2318. <https://doi.org/10.1016/j.cub.2016.06.034>
- Tuttle, E. M., Bergland, A. O., Korody, M. L., Brewer, M. S., Newhouse, D. J., Minx, P., Stager, M., Betuel, A., Cheviron, Z. A., Warren, W. C., Gonser, R. A., & Balakrishnan, C. N. (2016). Divergence and functional degradation of a sex chromosome-like supergene. *Current Biology*, 26, 344–350. <https://doi.org/10.1016/j.cub.2015.11.069>
- van der Auwera, G. A., & O'Connor, B. D. (2020). *Genomics in the cloud: Using Docker, GATK, and WDL in Terra*. O'Reilly Media.
- Vitalis, R., Gautier, M., Dawson, K. J., & Beaumont, M. A. (2014). Detecting and measuring selection from gene frequency data. *Genetics*, 196(3), 799–817. <https://doi.org/10.1534/genetics.113.152991>
- Walsh, J., Billerman, S. M., Butcher, B. G., Rohwer, V. G., Toews, D. P. L., Vila-Coury, V., & Lovette, I. J. (2023). A complex genomic architecture underlies reproductive isolation in a north American oriole hybrid zone. *Communications Biology*, 6(1), 154. <https://doi.org/10.1038/s42003-023-04532-8>
- Wang, M.-S., Zhang, R.-W., Su, L.-Y., Li, Y., Peng, M.-S., Liu, H.-Q., Zeng, L., Irwin, D. M., Du, J.-L., Yao, Y.-G., Wu, D.-D., & Zhang, Y.-P. (2016). Positive selection rather than relaxation of functional constraint drives the evolution of vision during chicken domestication. *Cell Research*, 26(5), 556–573. <https://doi.org/10.1038/cr.2016.44>
- Wang, S., Rohwer, S., Zwaan, D. R., Toews, D. P. L., Lovette, I. J., Mackenzie, J., & Irwin, D. (2020). Selection on a small genomic region underpins differentiation in multiple color traits between two warbler species. *Evolution Letters*, 4, 502–515. <https://doi.org/10.1002/evl3.198>
- Wellenreuther, M., & Bernatchez, L. (2018). Eco-evolutionary genomics of chromosomal inversions. *Trends in Ecology & Evolution*, 33(6), 427–440. <https://doi.org/10.1016/j.tree.2018.04.002>
- Wellenreuther, M., Mérot, C., Berdan, E., & Bernatchez, L. (2019). Going beyond SNPs: The role of structural genomic variants in adaptive evolution and species diversification. *Molecular Ecology*, 28(6), 1203–1209. <https://doi.org/10.1111/mec.15066>
- Wellenreuther, M., Svensson, E. I., & Hansson, B. (2014). Sexual selection and genetic colour polymorphisms in animals. *Molecular Ecology*, 23(22), 5398–5414. <https://doi.org/10.1111/mec.12935>
- Westram, A. M., Rafajlović, M., Chaube, P., Faria, R., Larsson, T., Panova, M., Ravinet, M., Blomberg, A., Mehlig, B., Johannesson, K., & Butlin, R. (2018). Clines on the seashore: The genomic architecture underlying rapid divergence in the face of gene flow. *Evolution Letters*, 2(4), 297–309. <https://doi.org/10.1002/evl3.74>
- Whittingham, L. A., Dunn, P. O., Freeman-Gallant, C. R., Taff, C. C., & Johnson, J. A. (2018). Major histocompatibility complex variation and blood parasites in resident and migratory populations of the common yellowthroat. *Journal of Evolutionary Biology*, 31, 1544–1557. <https://doi.org/10.1111/jeb.13349>
- Whittingham, L. A., Freeman-Gallant, C. R., Taff, C. C., & Dunn, P. O. (2015). Different ornaments signal male health and MHC variation in two populations of a warbler. *Molecular Ecology*, 24(7), 1584–1595. <https://doi.org/10.1111/mec.13130>
- Yang, J., Qu, Y., Huang, Y., & Lei, F. (2018). Dynamic transcriptome profiling towards understanding the morphogenesis and development of diverse feather in domestic duck. *BMC Genomics*, 19(1), 391. <https://doi.org/10.1186/s12864-018-4778-7>
- Yazdi, H. P., & Ellegren, H. (2018). A genetic map of ostrich Z chromosome and the role of inversions in avian sex chromosome evolution. *Genome Biology and Evolution*, 10(8), 2049–2060. <https://doi.org/10.1093/gbe/evy163>
- Zhou, X., & Stephens, M. (2014). Efficient multivariate linear mixed model algorithms for genome-wide association studies. *Nature Methods*, 11(4), 407–409. <https://doi.org/10.1038/nmeth.2848>

## SUPPORTING INFORMATION

Additional supporting information can be found online in the Supporting Information section at the end of this article.

**How to cite this article:** Dunn, P. O., Sly, N. D., Freeman-Gallant, C. R., Henschen, A. E., Bossu, C. M., Ruegg, K. C., Minias, P., & Whittingham, L. A. (2024). Sexually selected differences in warbler plumage are related to a putative inversion on the Z chromosome. *Molecular Ecology*, 33, e17525. <https://doi.org/10.1111/mec.17525>